Myelin abnormalities in the optic and sciatic nerves of mice with GM1-gangliosidosis

Author: Karie A. Heinecke

Boston College

The Graduate School of Arts and Sciences

Department of Biology

MYELIN ABNORMALITIES IN THE OPTIC AND SCIATIC NERVES OF MICE WITH GM1-GANGLIOSIDOSIS

a Thesis

by

KARIE A. HEINECKE

submitted in partial fulfillment of the requirements

for the degree of

Master of Science

May 2014

MYELIN ABNORMALITIES IN THE OPTIC AND SCIATIC NERVES OF MICE WITH GM1-GANGLIOSIDOSIS

Karie A. Heinecke

Advisor: Thomas N. Seyfried, Ph.D.

ABSTRACT

GM1 gangliosidosis is a glycosphingolipid lysosomal storage disease caused by a genetic deficiency of acid β-galactosidase (β-gal), the enzyme that catabolyzes GM1 within lysosomes. Accumulation of GM1 and its asialo form (GA1) occurs primarily in the brain, leading to progressive neurodegeneration and brain dysfunction. Less information is available on the neurochemical pathology in optic nerve and sciatic nerve of GM1- gangliosidosis. Here we analyzed the lipid content and myelin structure in optic and sciatic nerve in 7 and 10 month old normal *β-gal* (+/?) and GM1-gangliosidosis *β-gal* (–/–) mice. Optic nerve weight was lower in the *β-gal* –/– mice than in unaffected *β-gal* +/? mice, but no difference was seen between the normal and the *β-gal* –/– mice for sciatic nerve weight. The concentrations of GM1 and GA1 were significantly higher in optic nerve and sciatic nerve in the *β-gal* –/– mice than in *β-gal* +/? mice. The content and composition of myelin-enriched cerebrosides, sulfatides, plasmalogen ethanolamines were significantly lower in optic nerve of *β-gal* –/– mice than in *β-gal* +/? mice, however cholesteryl esters were enriched in the *β-gal* –/– mice. No significant abnormalities in these myelin enriched lipids were detected in sciatic nerve of the *β-gal* –/– mice. The abnormalities in GM1 and myelin lipids in optic nerve of *β-gal* –/– mice were also associated with abnormalities in the X-ray

diffraction pattern including myelin content in fresh nerves [M/(M +B)] and periodicity (d). With the exception of a slight reduction in myelin content, no abnormalities in the X-ray diffraction pattern were observed in sciatic nerve of *β-gal* –/– mice. The results indicate that neurochemical pathology is greater in optic nerve than in sciatic nerve of *β-gal* –/– mice.

DEDICATION

To My Family: Michael, Marianna, and Evelyn Heinecke

My Parents: Dennis Berbach and Janet Berbach-Koehler

My Siblings: Mark, Denise, and Vincent Berbach

My Grandmother: Anna Siepiela

ACKNOWLEDGEMENTS

I express deep gratitude to Dr. Thomas N. Seyfried for acceptance into his laboratory and support throughout my graduate school career.

I thank Dr. Rena Baek and Dr. Christine Ann Denny for teaching me almost everything I know about lipid analysis in the Seyfried lab.

I am grateful to Dr. Daniel Kirschner for his allowing me to collaborate with his lab for X-ray diffraction on the mouse nerves. I thank Adrienne Loma for teaching me how to properly prepare nerves for XRD. I thank Adrienne and Michelle Crowther for assistance with collecting the diffraction data.

I thank Hannah Rockwell, Alexandra Gonzalez and Michaela Annunziato for assistance with nerve collection for lipid analysis.

I thank past and present members of the Seyfried lab for technical assistance and support, especially: Linh Ta, Dr. Purna Mukherjee, Dr. Julian Aurthur, Zeynep Akgoc, Dr. John Mantis, Dr. Michael Kiebish, and Dr. Leanne Huysentruyt.

For funding, I thank the National Tay-Sachs and Allied Disease Association, Inc., the National Institutes of Health Grant NS- 055195, Boston College Research Expense Fund, and the Boston College Graduate School of Arts and Sciences, and the American Society for Neurochemistry for providing funds to present my work at the American Society for Neurochemisty annual meeting.

LIST OF TABLES Page

LIST OF FIGURES Page

ABBREVIATIONS

Å	Angstrom
B	Background intensity
β-gal	β-galactosidase
BMP	bis(monoacylglycero)phosphate
C	Cholesterol
CE	Cholesteryl ester
CBL	Cerebroside – Lower band
CBU	Cerebroside – Upper band
CL	Cardiolipin
CH_3OH	Methanol
$CHCl_3$	Cloroform
Cer or CM	Ceramide
CGT	Ceramide galactosyltransferase
cm	Centimeters
CNS	Central nervous system
CST	Cerebroside sulfotansferase
d	the periodicity of the peaks
DNA	Deoxyribonucleic acid
ER	Endoplasmic reticulm
GA1	asialo-GM1
Gal	Galactose
GalCer	Galactosylceramide or Cerebroside
Gal*N*Ac	*N*-acetylgalactosamine
Gal-T1	Galactosyltransferase
Glc	Glucose
GlcCer	Glucosylceramide
Glc-T	Glucosyltransferase
GM2AP	GM2 activator protein
GSD	Ganglioside storage disease
GSL	Glycosphingolipid

hFA	Hydroxy fatty acid
HPTLC	High performance thin-layer chromatogram
Jxp	Juxtaparanode
LacCer	Lactosylceramide
LPC	lysophosphatidylcholine
LSD	Lysosomal storage disease
L/U	Ratio of the lower band to the upper band
IS	Internal standard (oleoly alcohol)
M	Myelin intesity above background
M+B	Total intesity of diffraction pattern from myelin and background
M/M+B	Relative amount of myelin
MBP	Myelin basic protein
mg	milligrams
μg	micrograms
ml	milliliters
μl	microliters
N_2	Nitrogen gas
NANA	*N*-acetylneuraminic acid
NGNA	*N*-glycolylneuramic acid
Neo	Neomycin-resistant (gene product)
PA	Phosphatidic acid
PC	Phosphatidylcholine
PCR	Polymerase chain reaction
PE	Phosphatidylethanolamine
PI	Phosphatidylinositol
PLP	Proteolipid protein
PNS	Peripheral nervous system
PS	Phosphatidylserine
SA	Sialic acid
SAP-B	Saponisin b
SD	Standard Deviation

SE	Standard Error
SF	Solvent Front
SM	Sphingomyelin
Sulf	Sulfatide – Total
SFL	Sulfatide – Lower band
SFU	Sulfatide – Upper band
Solvent A	Chloroform:methanol:water, 30:60:8 by volume
Solvent B	Chloroform:methanol:0.8M sodium acetate, 30:60:8 by volume
Sph	Sphingosine
SpJ	Septate-like junction
Std	Standard
TG	Triglyceride
UDP	Uridine diphosphate
XRD	X-ray diffraction

CHAPTER ONE

INTRODUCTION

Glycosphingolipids

Lipids are important components of cellular membranes, responsible for separating the inside of the cell from the outside, selectively allowing molecules into and out of the cell, and communicating with neighboring cells (van Meer *et al.* 2008, Nature 2013, Bisel *et al.* 2014). Glycosphingolipids (GSL) are amphiphilic, and consist of an oligosaccharide head group attached to the lipophilic ceramide (D'Angelo *et al.* , Hakomori 1990, Lingwood 2011, Ledeen 1983) (Figure 1). Ceramide is comprised of a sphingosine base and a long-chain fatty acid. The addition of carbohydrates and other modifications to ceramide generate gangliosides, cerebrosides and sulfatides (D'Angelo *et al.* , Lingwood 2011, Kolter 2012, Kolter *et al.* 2002).

Lipids can provide important information about the integrity of the brain and nervous tissue. Gangliosides are sialic acid (SA) containing GSL residing in cell membranes, primarily in the nervous system (Yu *et al.* 2012, Schnaar RL *et al.* 2009, Ledeen 1983) (Figure 2). The oligosaccharide chain consists of different combinations of glucose, galactose, *N*-acetylgalactosamine, and *N*-acetylglucosamine (Ledeen 1983). SA residues are 9-carbon sugars, which are expressed in two forms, *N*-acetylneuraminic acid (NANA) or *N*-glycolylneuraminic acid (NGNA) and are attached to the galactose subunits of the oligosaccharide chain (Kawano *et al.* 1995, Davies *et al.*). The combination of the two different SA species, the number of SA species, the length of the oligosaccharide chain,

and the variation in the fatty acid chain length of the ceramide moiety contribute to the structural diversity of gangliosides (Yu *et al.* 2012, Ando *et al.* 1984, Ledeen *et al.* 1982, Sonnino *et al.* 2006). The ceramide portion of the GSL is anchored into the outer leaflet of the lipid bilayer and its oligosaccharide head group is projected into the extracellular environment (Figure 2).

The individual ganglioside species are differentially distributed in the different cell types of the brain (Wiegandt 1995, Vajn *et al.* 2013, Seyfried *et al.* 1984b, Seyfried *et al.* 1983). Ganglioside GT1a/LD1 is enriched in Purkinje cells, GD1a is enriched in granule cell neurons, and GT1b and GQ1b are enriched in both types of cerebellar nerve cells (Vajn *et al.* 2013, Seyfried *et al.* 1984a, Seyfried *et al.* 1983, Furuya *et al.* 1994, Chou *et al.* 1990, Seyfried *et al.* 1990). Ganglioside GM1, cerebrosides, and sulfatides are enriched in myelin membranes (Cuzner *et al.* 1968, Menkes *et al.* 1966, Suzuki *et al.* 1968a, O'Brien *et al.* 1965b, Vajn *et al.* 2013, Zalc *et al.* 1981, Muse *et al.* 2001, Coetzee *et al.* 1996, Yu *et al.* 1975). Cerebrosides and sulfatides are essential for proper myelination of axons (Marcus *et al.* 2006, Jackman *et al.* 2009, Hayashi *et al.* 2013).

Gangliosides have been shown to influence several important biological processes, such as cell adhesion, cell growth, angiogenesis, and signal transduction (Yu *et al.* 2012, Hakomori 1990, Bisel *et al.* 2014). Studies have also shown that gangliosides may interact with toxins, viruses, bacteria, as well as modulating membrane receptors (Singh *et al.* 2000, Sandhoff *et al.* 1994, Bisel *et al.* 2014).

GSL Synthesis and Degradation

Ceramide is converted into galactosylceramide (GalCer or cerebroside) or glucosylceramide (GlcCer) in the lumen of the endoplasmic reticulum (ER) (Kolter 2012, Kolter *et al.* 2002) (Figure 3). The cerebroside can then be sulfated on the luminal side of the Golgi apparatus to generate sulfatide, and GlcCer goes to the cytoplasmic side of the Golgi to begin biosynthesis of gangliosides (Lingwood 2011, Kolter 2012, Kolter *et al.* 2002). Completed lipids go to the cell membranes to provide their individual functions. During times of recycling, the membrane forms an endocytic vesicle, which becomes a lysosomal compartment used for molecular recycling (Figure 4).

Ganglioside synthesis occurs through the control of a complex of multi-glycosyltransferases and sialyltransferases (Figure 5) (Yu *et al.* 2012, Kolter *et al.* 2006). This process involves the synthesis of each ganglioside species on it own microsomal assembly where each metabolic intermediate becomes the substrate for the next biosynthetic reaction (Yu *et al.* 2012, Kolter *et al.* 2006). Following synthesis, gangliosides are packaged into vesicles, which bud off from the Golgi compartments, and travel to the cell surface, where they fuse with the plasma membrane (Yu *et al.* 2012, Kolter *et al.* 2006).

Ganglioside biosynthesis can be classified into four metabolic pathways, the “o”, “a”, “b”, and “c” pathways (Figure 5). Gangliosides synthesized through the “a”, “b”, and “c” pathways have one, two, and three sialic acids, respectively (Yu *et al.* 2012). In mammalian brain, the gangliosides in the “a” and “b” pathway

constitute the predominant species of gangliosides (Sandhoff *et al.* 2013, Yu *et al.* 2012). The “o” series of gangliosides begin without any sialic acid residues, also known as asialo-gangliosides, are prominent when the other pathways of ganglioside biosynthesis are disrupted (Yamashita *et al.* 2005, Yu *et al.* 2012). GM1, GD1a, GD1b, and GT1b are the major brain gangliosides in mature mammalian brains (Sturgill *et al.* 2012).

Ganglioside degradation also occurs in a stepwise fashion but in the reverse order of biosynthesis. Gangliosides are endocytosed from the plasma membrane and transported to the lysosome through various endosomal compartments (Wilkening *et al.* 2000, Yu *et al.* 2012, Kolter *et al.* 2006, Sandhoff *et al.* 2013). In the lysosomes, gangliosides are completely or partially degraded by the sequential removal of individual sugar residues by substrate-specific acidic hydrolytic enzymes and activator proteins (Yu *et al.* 2012, Kolter *et al.* 2006, Sandhoff *et al.* 2013). The by-products of degradation, sugars (glucose, galactose, hexosamine), lipids (ceramide, sphingosine, and fatty acid), and sialic acid residues are recycled to the Golgi for lipid biosynthesis and re-glycosylation (Yu *et al.* 2012, Kolter *et al.* 2006, Sandhoff *et al.* 2013).

Ganglioside Storage Disease

Lysosomal storage diseases (LSD) are characterized by the accumulation of macromolecules in the lysosomal compartment due to defects in catabolic enzymes or their activator proteins (Kolter *et al.* 1998). Over 40 different types of LSD have been described to date, and all together, they affect 1 in 7,000 live-

born infants per year (Meikle *et al.* 1999). Most inherited diseases of GSL metabolism in humans affect the hydrolytic pathways, instead of the synthetic pathways (Kolter *et al.* 2006, Kolter *et al.* 1998, Xu *et al.* 2010). However, in the past decade multiple disruptions to different synthase activities have been shown, though their occurrence in nature is still very rare (Boukhris *et al.* 2013, Yu *et al.* 2012, Yao *et al.* 2014, Yamashita *et al.* 2005, Xu *et al.* 2010, Staretz-Chacham *et al.* 2009, Schnaar 2010, Jennemann *et al.* 2005, Harlalka *et al.* 2013, Freeze *et al.* 2011).

GM1-gangliosidosis is a type of LSD, or ganglioside storage diseases (GSD), caused by an autosomal recessive deficiency of lysosomal acid β-galactosidase (*β-gal*) (Figure 6). Deficiency of the lysosomal enzyme leads to accumulation of GM1 ganglioside, and its asialo-derivative, in neuronal and non-neuronal tissue, followed by progressive neurodegeneration (Hahn *et al.* 1997, Saunders *et al.* 1988, Matsuda *et al.* 1997a, Landing *et al.* 1964, Lyon GL *et al.* 1996, O'Brien *et al.* 1965c, NINDS 2011, Suzuki *et al.* 2001, Baek *et al.* 2010). The most severe form of this disease (Infantile or Type I) has a very early onset, and is characterized by rapid neurological deterioration with death usually occurring before 3 years of age, in humans (NINDS 2011). There is currently no effective treatment for GM1- gangliosidosis. In addition to humans, the diseases can be found in other animals, including dog, cat, and American black bear (Muthupalani *et al.* 2014, Suzuki *et al.* 1968b, Read *et al.* 1976, Baker *et al.* 1974, Karbe 1973, Baker *et al.* 1976).

GM1 catabolism occurs through the concerted actions of β-galactosidase (*β-gal* or *GLB1*) and an activator protein, either saponisin b or GM2 activator protein (GM2AP) (Figure 7) (Wilkening *et al.* 2000). GM1 gangliosidosis results from inherited defects in the *β-gal* gene and is estimated to occur in every 100,000-200,000 live human births (Sinigerska *et al.* 2006). Generalized gangliosidosis or GM1 gangliosidosis was first described in the late 1950's – early 1960's (Norman *et al.* 1959, Craig *et al.* 1959, Landing *et al.* 1964). It wasn't until 1968 that the biochemical deficiency in GM1 gangliosidosis was explained (Okada *et al.* 1968). The onset of disease ranges from infancy to adulthood, which correlates with relative β-gal activity. In the infantile form, presentation of the disease is associated with rapid motor deterioration, macular cherry red spot, and skeletal dysplasia (Folkerth *et al.* 2000). Pathogenesis in GM1 gangliosidosis is marked with neuronal damage or death, inflammation, and progressive neurological deterioration (van der Voorn *et al.* 2004, Folkerth *et al.* 2000). Ocular abnormalities involving membranous cytoplasmic bodies, ganglion cell loss and optic nerve atrophy have been characterized in patients with GM1 gangliosidosis (Denny *et al.* 2007, Cairns *et al.* 1984). In addition, myelin abnormalities in the human patients are also seen in the cat, dog, and mouse disease models (Kroll *et al.* 1995, Folkerth *et al.* 2000, van der Voorn *et al.* 2004, Kaye *et al.* 1992).

Mouse Model of GM1 Gangliosidosis

The available knockout mouse models replicate many features of GM1-gangliosidisis, infantile, in humans; including, biochemical deficiency, the neurochemical accumulation, and the pathological consequence loss of gross motor skills, blindness, and alterations in brain lipids (Matsuda *et al.* 1997a, Suzuki *et al.* 2001, Baek *et al.* 2010, Hahn *et al.* 1997, Matsuda *et al.* 1997b, Tessitore *et al.* 2004). Mice lacking β-gal activity was generated using homologous recombination and embryonic stem cell technology (Matsuda *et al.* 1997b, Hahn *et al.* 1997). The *β-gal* -/- mice express residual β-gal activity and elevation of GM1 and GA1, mimicking the infantile form of GM1 gangliosidosis. GA1 accumulation is greater in the mouse model than in patients with GM1 gangliosidosis most likely because of a more active sialidase specific to this substrate (Hahn *et al.* 1997). Despite CNS GM1 accumulation from as early as postnatal day 5, the *β-gal* -/- mice do not show behavioral abnormalities until adult ages (Kasperzyk *et al.* 2004, Matsuda *et al.* 1997a). In contrast to infantile onset patients, where ganglioside accumulation leads to behavioral and developmental abnormalities within the first few years of life, β-gal-deficient mice are phenotypically indistinguishable from normal mice until adult ages (Hahn *et al.* 1997). The *β-gal* -/- mice display ataxia, hind limb paralysis, and difficulty in walking and can be used to study GM1 gangliosidosis (Baek *et al.* 2010, Hahn *et al.* 1997). Previous studies have shown major alterations to brain gangliosides, cerebrosides and sulfatides in *β-gal* -/- mice, which recapitulate lipid levels in humans with GM1-gangliosidosis (Hahn *et al.* 1997, Suzuki *et al.* 2001, O'Brien *et al.* 1965b, Baek *et al.* 2010, Matsuda *et al.* 1997b).

Myelin

Myelin is a specialized membrane of nervous tissue, which differs from other membranes in the CNS (i.e. grey matter or white matter), due to a higher amount of lipids, compared to other membrane components (O'Brien *et al.* 1965b). Oligodendrocytes and Schwann cells share a common function of insulating axons with myelin, however one resides in the CNS and the other in the PNS, respectively (Kettenmann *et al.* 2011). The myelin membrane is generated by an extension of the oligodendrocyte or Schwann cell plasma membrane that tightly wraps around a portion (~0.4-1.4mm) of the axon (Asbury 1975, Kettenmann *et al.* 2011) (Figures 8 & 9). Oligodendrocytes are able to myelinate up to 40 different axons, while Schwann cells are able to myelinate one axon at a time. Myelin insulates the axonal segments to enable high velocity nerve conduction. In humans, myelination begins *in utero* at the spinal cord with peak activity the first year after birth, and continues until approximately 20 years of age (Kettenmann *et al.* 2011). In rodents, myelination begins at birth and is primarily completed at approximately 2 months after birth (Kettenmann *et al.* 2011). Primary myelination is completed early in development, however the amount of myelin in humans and rodents continue to increase with age in the CNS, but has been observed to decrease in age in human peripheral nerves (Cuzner *et al.* 1968, Spritz *et al.* 1973, Menkes *et al.* 1966, Yu *et al.* 1975, Horrocks 1973, Kettenmann *et al.* 2011). Even with an increase or decrease in myelin content, the myelin composition tends to remains stable (Clausen *et al.*

1970, Nussbaum *et al.* 1971, O'Brien *et al.* 1965a, Spritz *et al.* 1973, Horrocks 1973). Oligodendrocyte progenitor cells are present in the mature brain and are a source for re-myelination in brains with myelin damage (Gumpel *et al.* 1989, Watzlawik *et al.* 2010).

Myelin degeneration and neurological deficits are observed in mice lacking complex gangliosides (GM1, GD1a, GD1b, GT1a, GT1b, and GQ1b) (Sheikh *et al.* 1999, Vyas *et al.* 2001, Chiavegatto *et al.* 2000, Jackman *et al.* 2009). In myelinated nerves of the CNS and PNS, gangliosides GD1a and GT1b reside in the plasma membrane of axons and associate with protein in the myelin membrane to provide stability and inhibit neuronal growth (Vyas *et al.* 2002, Jackman *et al.* 2009). Ganglioside GM1 is enriched in myelin at the axolemma and nodes of Ranvier and has been used to indicate myelin content in previous studies (Ganser *et al.* 1984, Seyfried *et al.* 1984b, Seyfried *et al.* 1984a, Seyfried *et al.* 1980, Muse *et al.* 2001, Suzuki *et al.* 2001, MacBrinn *et al.* 1969). The brains of animals and humans with GM1 gangliosidosis have shown myelinating defects (Nada *et al.* 2011, van der Voorn *et al.* 2005, Muller *et al.* 2001, Brunetti-Pierri *et al.* 2008, van der Voorn *et al.* 2004, Gururaj *et al.* 2005, Di Rocco *et al.* 2005, Shen *et al.* 1998, Kasama *et al.* 1986, Kaye *et al.* 1992, Folkerth *et al.* 2000). Animals with GM1-gangliosidosis show a reduction in lipids enriched in myelin, myelin degradation and neuronal degradation.

X-ray diffraction (XRD) is a useful technique in determining the periodicity of myelin, the relative amounts of myelin, and myelin membrane packing defects in freshly dissected nerves (Yin *et al.* 2006, Schmitt *et al.* 1935, Kirschner *et al.* 2010, Avila *et al.* 2005). XRD was useful in identifying myelin membrane packing abnormalities in the nerves of animals with myelinating disorders (Avila *et al.* 2010, Kirschner *et al.* 2010, Kirschner *et al.* 1976, Appeldoorn *et al.* 1975, Ruocco *et al.* 1984, Mateu *et al.* 1991, Inouye *et al.* 1985, Chia *et al.* 1984, Brown *et al.* 1985, Blaurock *et al.* 1991, Karthigasan *et al.* 1996, Kirschner *et al.* 1996, Vargas *et al.* 1997, Vonasek *et al.* 2001, Avila *et al.* 2005, Yin *et al.* 2006, McNally *et al.* 2007). Using XRD, McNally *et al*., found a reduction in the amount of myelin in optic nerves of Sandhoff mice, but no abnormalities in sciatic nerves (McNally *et al.* 2007). While many LSD display PNS accumulation, McNally *et al.* was the first to assess myelin based on XRD. This is the first assessment of the myelin in GM1 gangliosidosis mice based on XRD. Histological and imaging studies on GM1 gangliosidosis in humans suggest various neuropathies in the PNS, but it is unclear the amount of PNS involvement associated in the phenotype of mice with GM1-gangliosidosis (Iwamasa *et al.* 1987, NINDS 2011, Read *et al.* 1976, Yamano *et al.* 1983, Shapiro *et al.* 2008, Jain *et al.* 2010, Mondelli *et al.* 1989).

Ganglioside GM1, cerebrosides and sulfatides have long been used as markers for myelin content and composition (O'Brien *et al.* 1965b, Zalc *et al.* 1981, Coetzee *et al.* 1996, Yu *et al.* 1975, Muse *et al.* 2001). Previous lipid

analyses in the brains of GM1-gangliosidosis mice have shown alterations to these myelin-enriched lipids (Baek *et al.* 2010, Yu *et al.* 1975, Hauser *et al.* 2004, Kasperzyk *et al.* 2004, Kasperzyk *et al.* 2005, Broekman *et al.* 2007). In addition, cholesteryl esters and plasmalogen ethanolamines, in humans, have also been altered, while other LSD animals with myelin defects (e.g. adrenoleukodystrophy and Niemann-Pick disease) are known to have abnormalities in these myelin lipids and cholesterol (Paintlia *et al.* 2003, Anchisi *et al.* 2013, Farooqui *et al.* 2001, Kasama *et al.* 1986, Suzuki *et al.* 1968b). Animals with GM1-gangliosidosis are known to have myelin defects (Nada *et al.* 2011, van der Voorn *et al.* 2005, Kasama *et al.* 1986, Kaye *et al.* 1992, Folkerth *et al.* 2000). Electron microscopy and histopathology on GM1-gangliosidosis brains have shown reduction in the amount of nerves present in different brain regions (van der Voorn *et al.* 2005, Tessitore *et al.* 2004). It has been shown that storage material in the nerves of GM1-gangliosidosis mice lead to endoplasmic reticulum (ER) distress, and apoptosis in neurons of the CNS and PNS (Tessitore *et al.* 2004, Lupachyk *et al.* , Platt *et al.* 2012). Increases in both cholesteryl esters and lysoplasmalogen ethanolamines (from the hydrolysis of plasmalogen ethanolamines) are also known to lead to ER distress and apoptosis (Farooqui *et al.* 2006, Farooqui *et al.* 2001). While abnormalities in lipid metabolism have a role in increased inflammation in the brain, inflammation has been shown to play a role in disease progression in GM1-gangliosidosis mice (Chrast *et al.* 2011, Jeyakumar *et al.* 2003).

The goal of this study was to determine if the content and composition of lipids and myelin structure were altered in optic and sciatic nerves in *β-gal* -/- mice. The results presented here indicate that previously observed changes in the CNS lipids enriched in myelin are expressed, in a qualitative and quantitative manner, in the optic and sciatic nerves of mice with GM1-gangliosidosis. Both optic and sciatic nerves of *β-gal* -/- mice had a reduction in the amount of myelin, an increase in ganglioside GM1, and the presence of the asialo form of GM1 (GA1). The optic nerves of *β-gal* -/- mice had additional lipid and myelin abnormalities. These data suggest that deficiency of GM1 β-galactosidase has a larger effect primarily on myelin in optic nerves then in sciatic nerves. The combination of lipid analysis and XRD provide a greater understanding of the neurochemical pathologies in GM1-gangliosidosis on the nerves of the CNS and PNS, especially in its relation to the ocular phenotype (blindness, discoloration of the fovea, and optic neuropathy) of the disease.

Figure 1. *De novo* synthesis of glycosphingolipids: sphingosine combines with fatty-CoA or hydroxyl fatty acid (hFA) to form ceramide, Glucose transfers to the ceramide to generate glucosylceramide (GlcCer), Galactose transfers to the GlcCer to generate lactosylceramide (LacCer) additional carbohydrates and sialic acids are added in a step wise fashion as the lipid travels through the Golgi on its way to the plasma membrane (5). Alternatively, galactose is transferred to the terminal hydroxyl residue of ceramide to generate galactosylceramide (GalCer), and a sulfhydryl group is added to the galactose residue to generate Sulfatide. The hFA is labeled in blue to designate that it is an optional addition. While hydroxylation is not common in most lipids, hydroxylated cerebrosides and sulfatide are enriched in myelin membranes. Abbreviations: PAPS, 3'-phospoadenosine-5'-phosphosulfate; CGT, Ceramide galactosyltransferase; CST, Cerebroside sulfotransferase; UDP, Uridine diphosphate; GalCer, Galactosylceramide; GlcCer, Glucosylceramide; LacCer, Lactosylceramide; Glc-T, Glucosyltransferase; Gal-T1, Galactosyltransferase; hFA, hydroxyl fatty acid. (Created by Karie A. Heinecke)

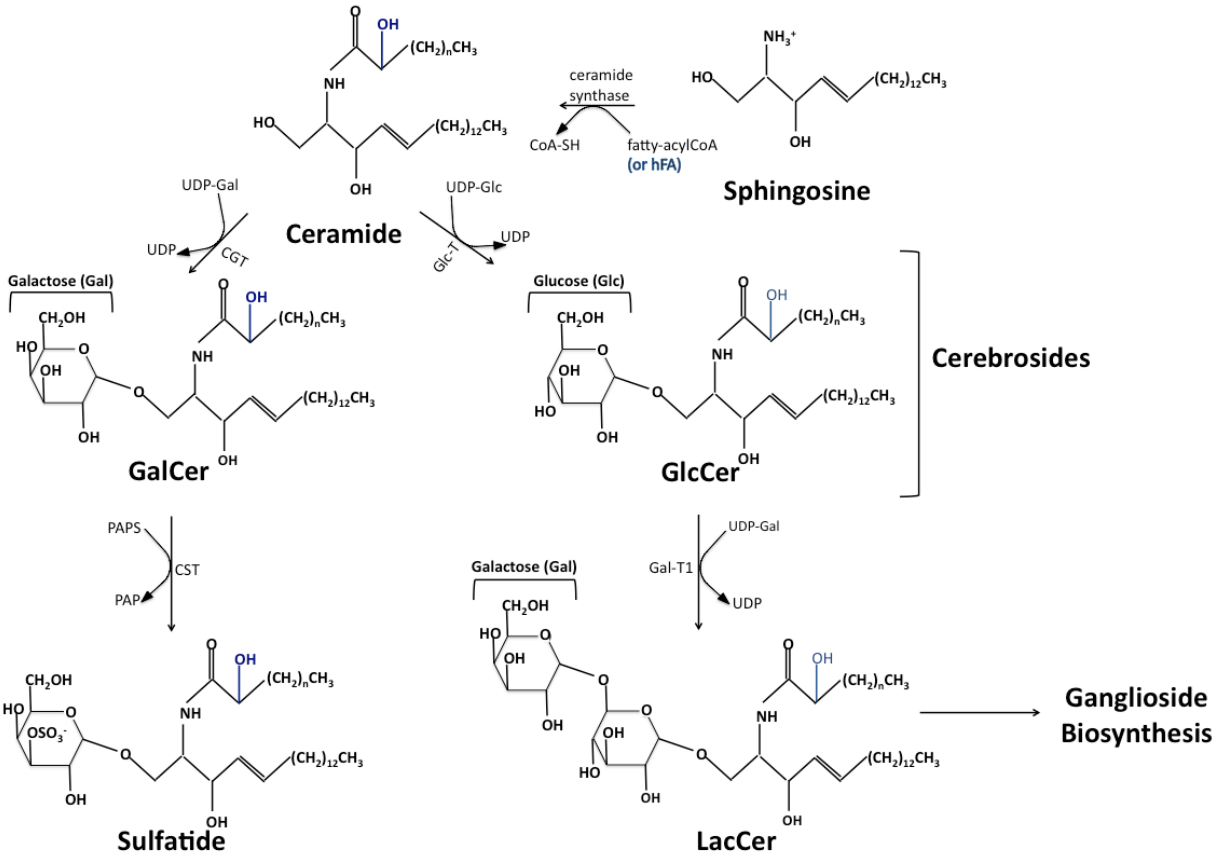
ceramide synthase
CoA-SH
fatty-acylCoA (or hFA)
Sphingosine
Ceramide
UDP-Gal
UDP
CGT
UDP-Glc
Glc-T
UDP
Galactose (Gal)
GalCer
Glucose (Glc)
GlcCer
Cerebrosides
PAPS
CST
PAP
Sulfatide
Galactose (Gal)
UDP-Gal
Gal-T1
UDP
LacCer
Ganglioside Biosynthesis

Figure 2. Ganglioside structure and orientation in the plasma membrane. The ceramide (Cer) portion inserts into the plasma membrane while the oligosaccharide head group extends into the extracellular environment. The roman numerals represent individual sugar residues that make up the GSL oligosaccharide chain: I = glucose, II = galactose, III = *N*-acetylgalactosamine, and IV = galactose. The letters A, B, and C represent sialic acid residues. Modified from (Ledeen *et al.* 1982)

Gangliosides	NGSLs
GM3: I, II, A	GlcCer: I
GM2: I, II, III, A	GalCer: II
GM1a: I, II, III, IV, A	LacCer: I, II
GM1b: I, II, III, IV, B	Gg3Cer: I, II, III
GD1a: I, II, III, IV, A, B	Gg4Cer: I, II, III, IV

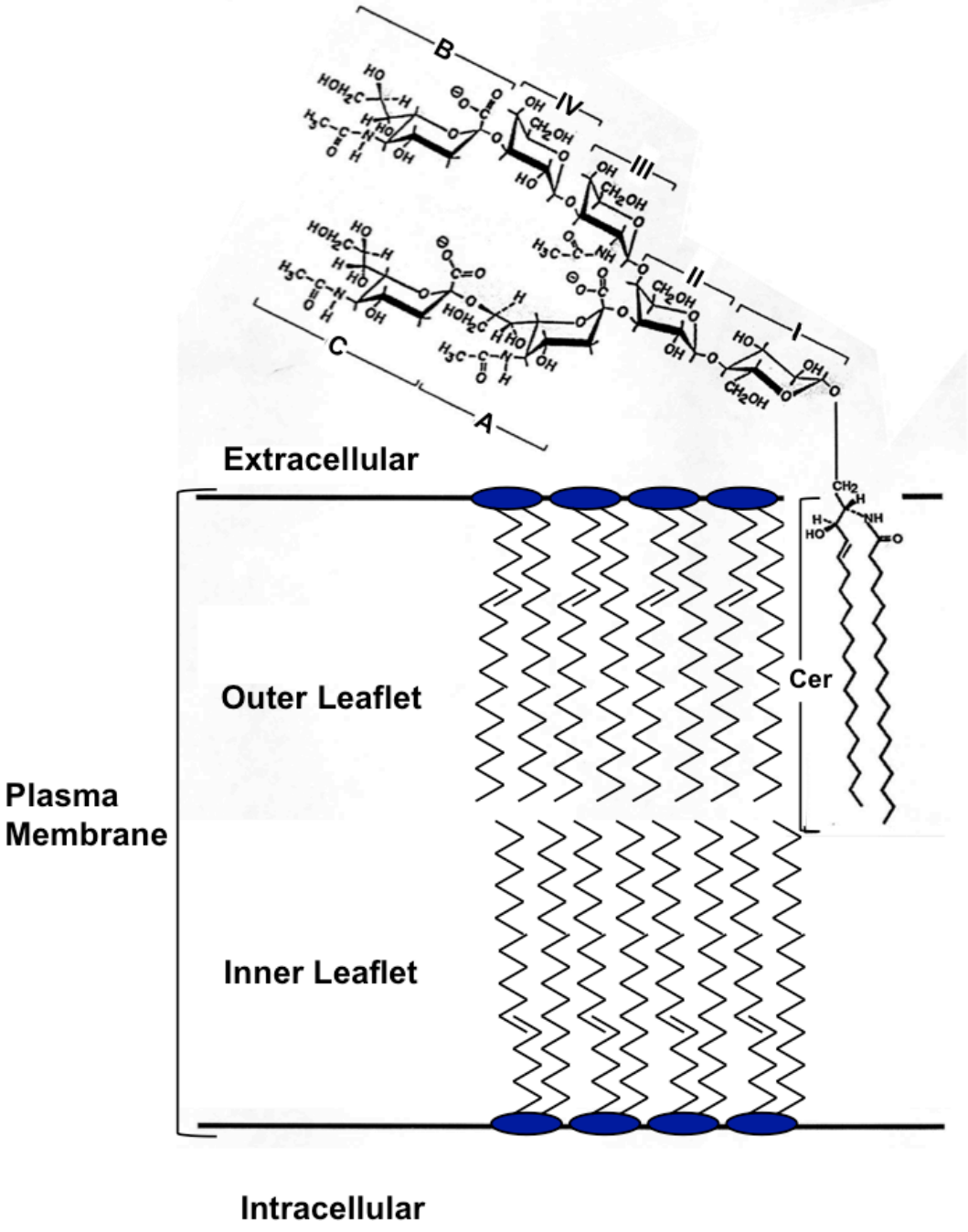

Figure 3. Organelle localization during lipid biosynthesis. De novo synthesis of glycosphingolipids: on the cytosolic side of the endoplasmic reticulum (ER) sphingosine combines with a fatty-CoA to form ceramide (1), ceramide moves from the ER to the cytosolic side of the Golgi (2), Glucose transfers to the ceramide to generate glucosylceramide (GlcCer) (3), a flippase moves the GlcCer to the Golgi lumen (4), where additional carbohydrates and sialic acids are added in a step wise fashion as the lipid travels through the Golgi on its way to the plasma membrane (5). Alternatively, ceramide (1) can be transported to the ER lumen (6) where a galactose is transferred to its terminal hydroxyl residue to generate galactosylceramide (GalCer) (7), GalCer moves to the Golgi lumen (8) where a sulfhydryl group is added to the galactose residue to generate Sulfatide (9). The cerebroside and sulfatide can be transported to the plasma membrane (10,11). Abbreviations: Sph, sphingosine; GSL, glycosphingolipids; Cer, Ceramide; GlcCer, glucosylceramide; GalCer, galactosylceramide; Sulf, sulfatide.

(Created by Karie A. Heinecke)

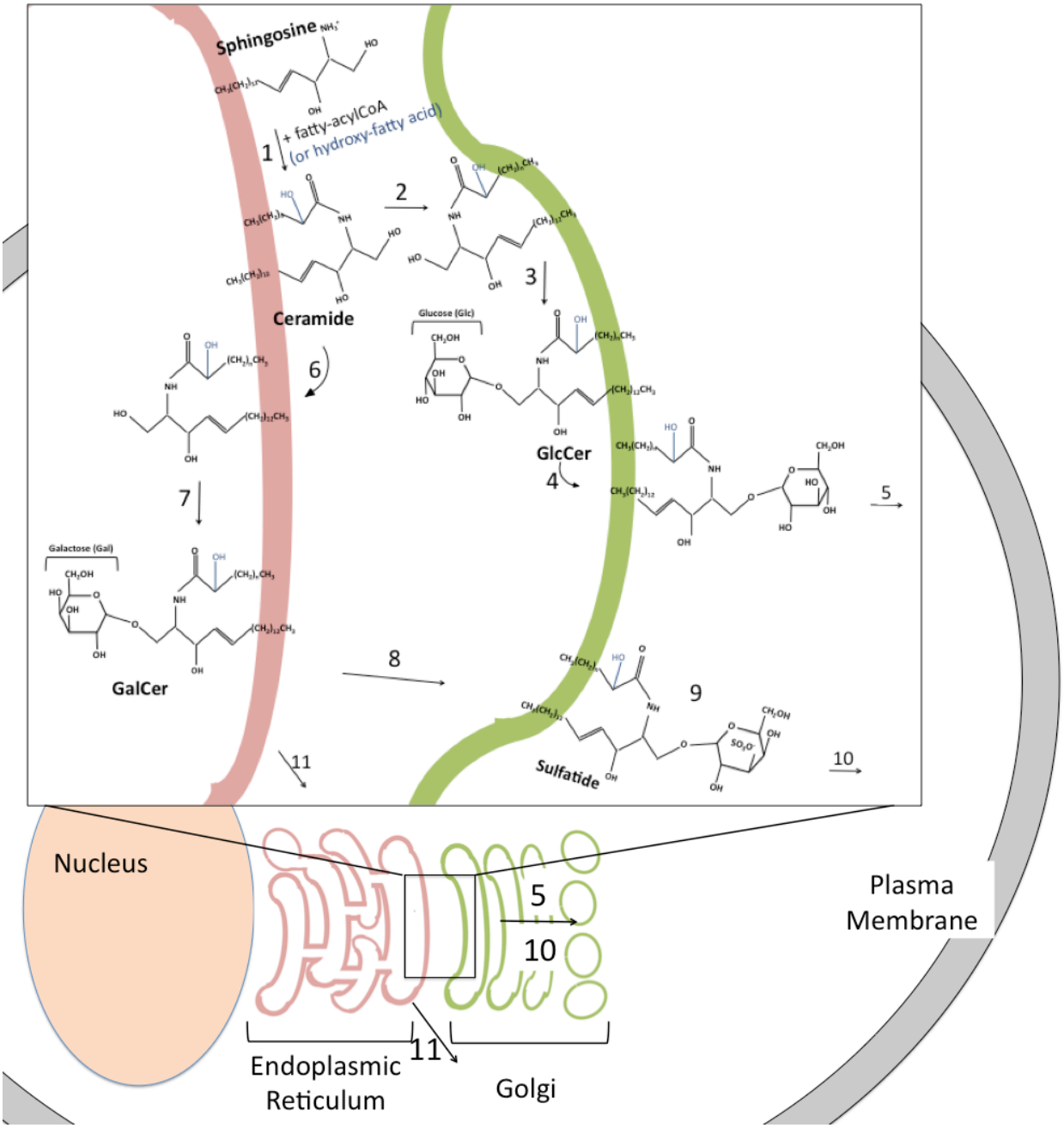
Sphingosine
1
+ fatty-acylCoA
(or hydroxy-fatty acid)
2
3
Ceramide
Glucose (Glc)
GlcCer
4
5
6
7
Galactose (Gal)
GalCer
8
9
Sulfatide
10
11
Nucleus
Plasma
Membrane
5
10
11
Endoplasmic
Reticulum
Golgi

Figure 4. Ganglioside/glycosphingolipid metabolic turnover: (a) chemical modifications (glycosylations / de-glycosylations) at the plasma membrane, (b) exogenous uptake of gangliosides, (c) direct recycling to the plasma membrane from endosomes, (d) sorting to the Golgi for direct glycosylation, (e) lysosomal degradation, (f) salvage processes at the ER and Golgi, (g) complete degradation of lipid products, (h) *de novo* biosynthesis from the ER and Golgi. (Created by Karie A. Heinecke)

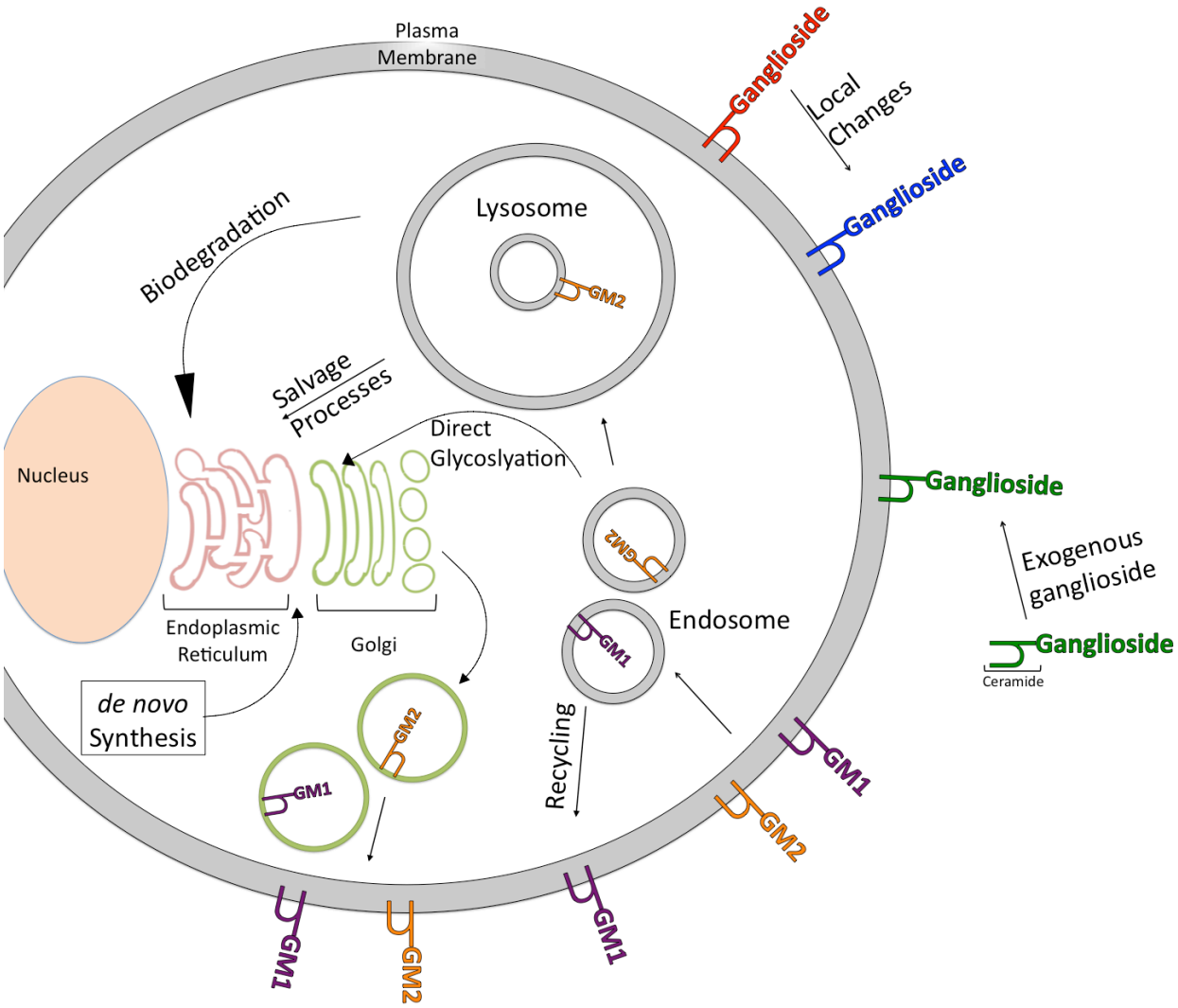
Plasma
Membrane
Ganglioside
Local
Changes
Ganglioside
Lysosome
GM2
Biodegradation
Salvage
Processes
Direct
Glycoslyation
Nucleus
Ganglioside
Exogenous
ganglioside
Endoplasmic
Reticulum
Golgi
GM2
Endosome
GM1
Ganglioside
Ceramide
de novo
Synthesis
GM2
GM1
Recycling
GM1
GM2
GM1
GM2
GM1

Figure 5. Ganglioside Biosynthetic Pathway.

GSL biosynthesis begins with the addition of glucose residues to ceramide to form glucosylceramide (GlcCer). Ganglioside biosynthesis proceeds by the action of multiple glycosyltransferases (black arrows) and sialyltransferases (red arrows), where the product of one enzymatic reaction is the substrate for the next biosynthetic reaction. Ganglioside synthesis is divided into three major metabolic pathways, the “a”, “b”, and “c” pathways. In addition, the “o” pathway consists of neutral GSL and gangliosides. Abbreviations: Glc, glucose; Gal, galactose; Gal*N*Ac, *N*-acetylgalactosamine; SA, sialic acid.

Modified from (Bieberich *et al.* 1999)

Glycosphingolipid Biosynthetic Pathways

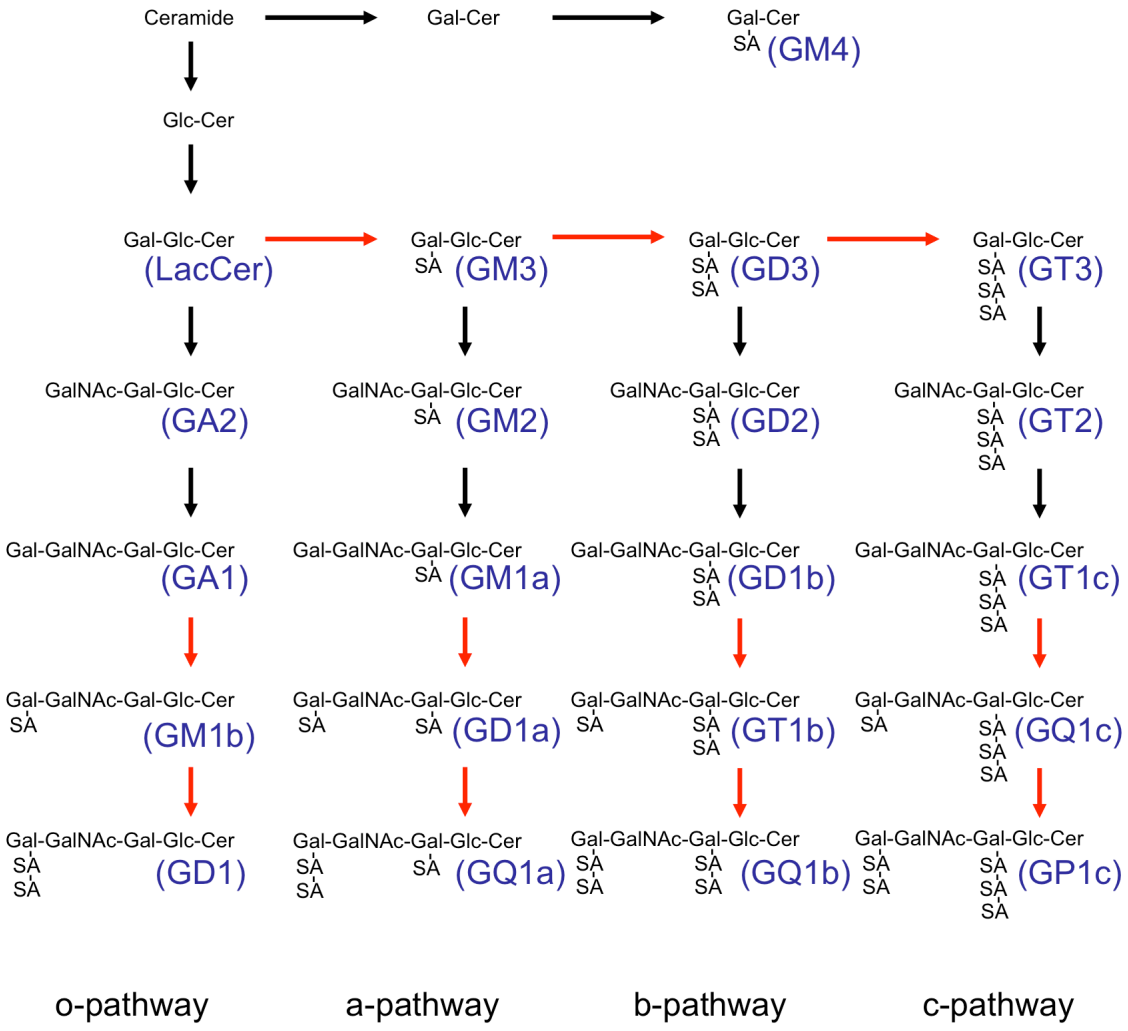

Figure 6. GM1 ganglioside.

Gangliosides are sialic acid (SA) containing GSL residing in cell membranes, primarily in the nervous system. The oligosaccharide chain consists of different combinations of glucose, galactose, *N*-acetylgalactosamine, *N*-acetylglucosamine, and sialic acid attached to a ceramide backbone. β-galactosidase hydrolyzes the terminal galactose from ganglioside GM1. Modified from (Salmond *et al.* 2002)

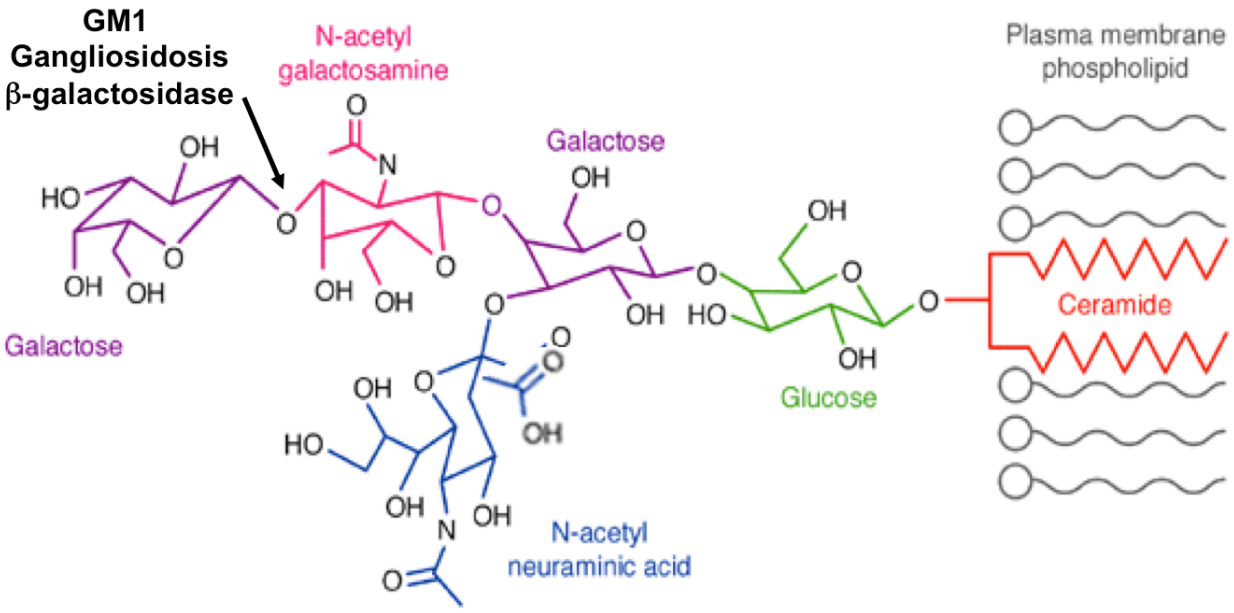

Structure of the membrane glycolipid G_{M1}

Figure 7. Model for the Lysosomal Degradation of Membrane-Bound GM1.

GM1 β-galactosidase binds to the negatively charged surface of intralysosomal vesicles at an acidic pH. The sphingolipid activator protein (SAP), either GM2AP (GM2 activator protein) or sap-b, associates with the bis(monoacylglycero) phosphate (BMP) in the intralysosomal membrane to remove GM1 from the membrane and present it to β-galactosidase.

Modified from (Wilkening *et al.* 2000)

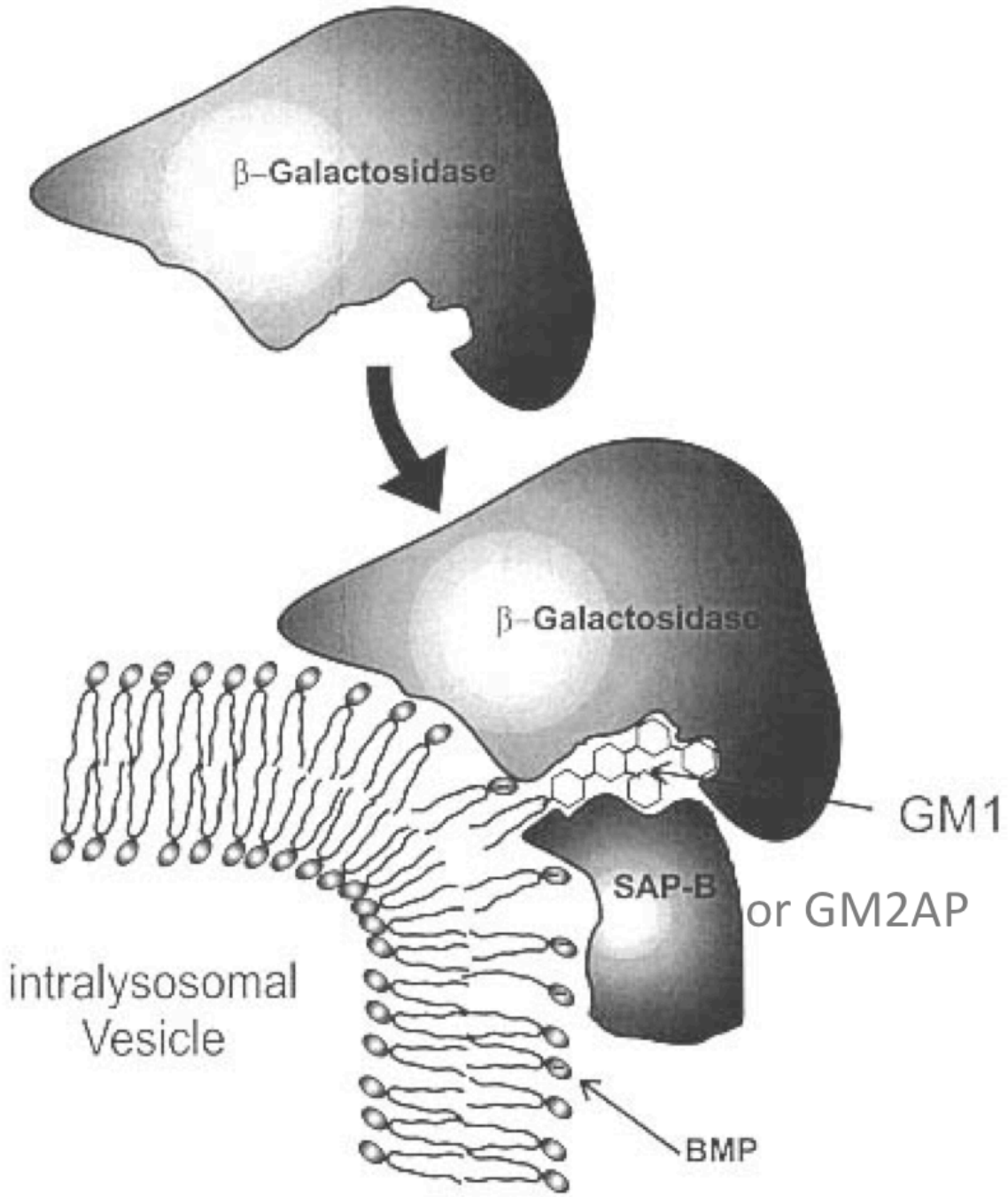
β–Galactosidase
β–Galactosidase
GM1
SAP-B
or GM2AP
intralysosomal
Vesicle
BMP

Figure 8. The Structure of Myelinated Axons. a. Myelinating glial cells form the myelin sheath by wrapping several times around the axon. Oligodendrocytes can myelinate many different axons in the CNS, while Schwann cells can myelinate one internode of a single axon in the PNS. b. Schematic longitudinal cut of a myelinated fiber near the node of Ranvier. The internode, juxtaparanode (JXP), paranode, and node are labeled. The node interacts with astrocytes in the CNS and Schwann cell microvilli in the PNS. The paranodal loops form septate-like junctions (SpJ) with the axon.

Modified from (Poliak *et al.* 2003)

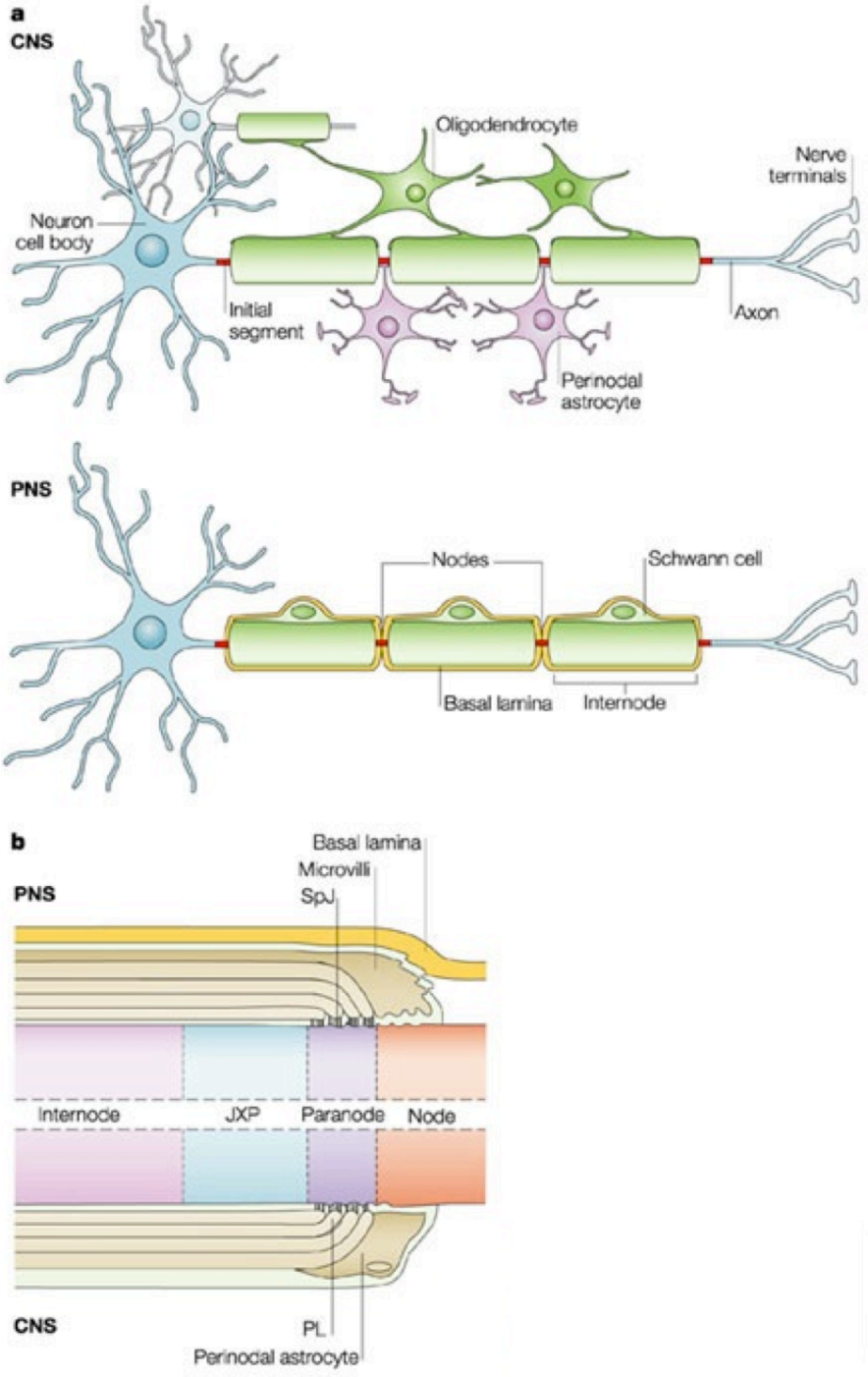
a
CNS
Oligodendrocyte
Nerve terminals
Neuron cell body
Initial segment
Axon
Perinodal astrocyte
PNS
Nodes
Schwann cell
Basal lamina
Internode
b
Basal lamina
Microvilli
PNS
SpJ
Internode
JXP
Paranode
Node
CNS
PL
Perinodal astrocyte

Figure 9. The Structure of the Myelin Sheath. A. The axon contains multiple nodes and internodes of myelinated and unmyelinated sections, respectively. B. The myelinated internode is an extension of the oligodendrocyte (CNS) or Schwann cell (PNS) membrane, which wraps around the axon. C. Each bilayer is separated by cytoplasmic and extracellular gaps where myelin specific proteins hold the layers in a compact formation (MBP, myelin basic protein; PLP, proteolipid protein). D. The myelin membrane is composed of many different lipids, including: phospholipids, glycosphingolipids, and cholesterol.
Modified from (Min *et al.* 2009)

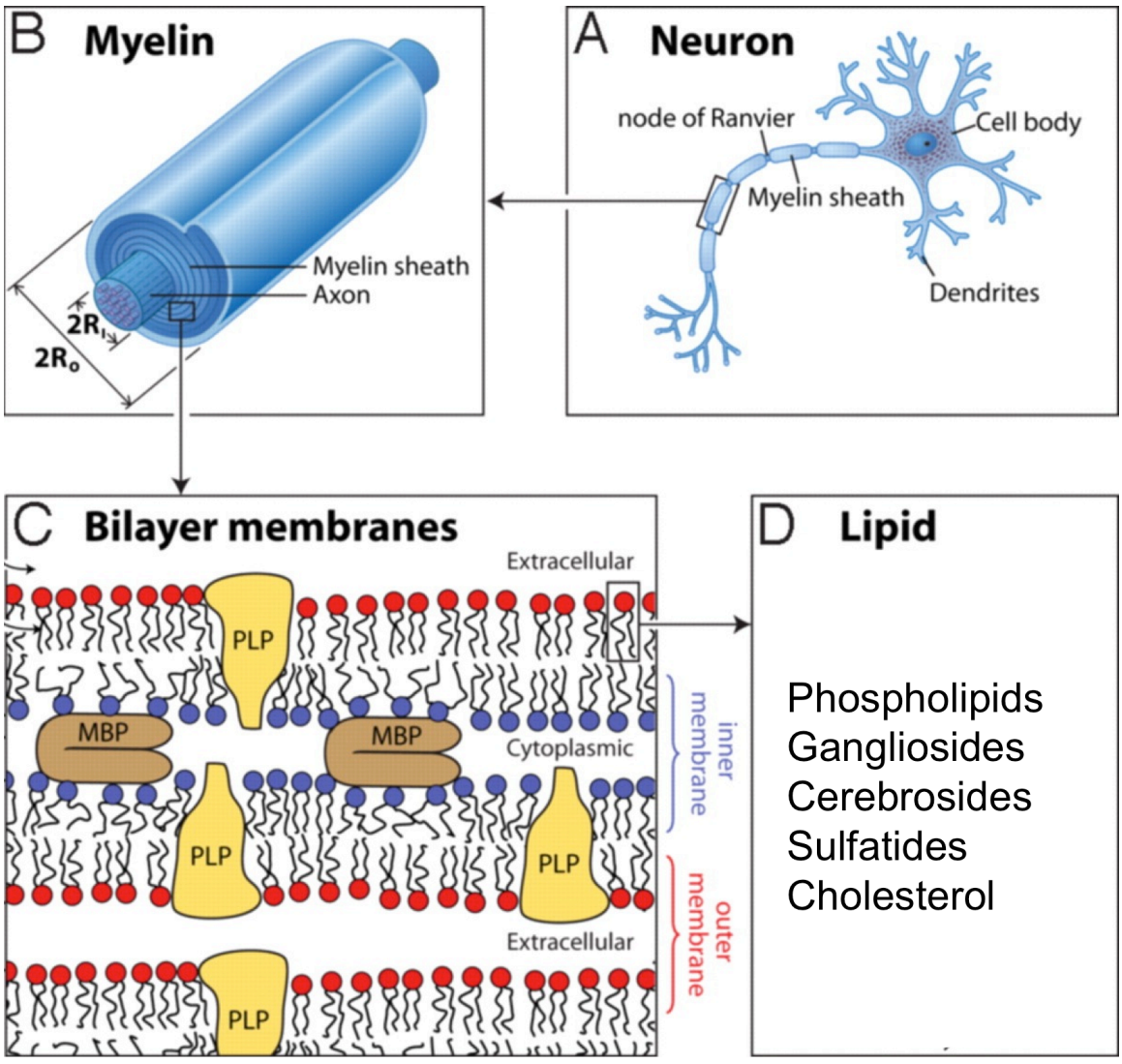
B Myelin
Myelin sheath
Axon
2R_i
2R_o
A Neuron
node of Ranvier
Cell body
Myelin sheath
Dendrites
C Bilayer membranes
Extracellular
PLP
MBP
MBP
Cytoplasmic
PLP
PLP
Extracellular
PLP
inner membrane
outer membrane
D Lipid
Phospholipids
Gangliosides
Cerebrosides
Sulfatides
Cholesterol

CHAPTER TWO

Materials and Methods

Animals

B6/129Sv mice heterozygous for the β-galactosidase gene (*β-gal* +/-) were obtained from Saint Jude Children's Research Hospital, Nashville, TN, USA (Dr. A. d'Azzo). These mice were generated independently by homologous recombination and embryonic stem cell technology, as previously described (Hahn *et al.* 1997). Sibling matings of mice heterozygous for the *β-gal* knockout allele (+/-) were used to produce *β-gal* -/- mice. Male and female wild type mice (+/+) and heterozygous mice (+/-) were used as controls (+/?). The mice were maintained through brother-sister inbreeding and kept in the Animal Care Facility of Boston College with all procedures in strict adherence with the NIH guide for the care and use of laboratory animals and approved by the Institutional Animal Care and Use Committee. The mice were housed in plastic cages with Sani-chip bedding (P.J. Murphy Forest Products Corp., Montville, N.J.) and kept on a 12-hr light/dark cycle at approximately 22°C. All cages and water bottles were changed once per week.

Mouse Genotyping

DNA was isolated from ~2 mm of mouse tail using the Wizard Genomic DNA purification Kit (Promega, Madison, WI) tail tissue protocol. PCR

amplification was performed using 1 µL of DNA (~50 - 100 ng). The PCR amplification of the *β-gal* gene was set up as follows: 5 µL of 5x GoTaq Buffer, 0.3 µL dNTPs (10 mM mix), 10 µM *β-gal* gene forward primer (5'-ACACACAGGTTGAGAATGAGTACGG-3'), 10 µM *β-gal* reverse primer (5'-ACACACACCGACCTGTTCCAAAATC-3), 10 µM neomycin-resistant (*Neo*) gene forward primer (5'-GTCACGACGAGATCCTCGCCGTC-3'), 10 µM *Neo* gene reverse primer (5'-GTCCGGTGCCCTGAATGAACTGC-3), 0.25 µL GoTaq DNA Polymerase (Promega), and brought up to 25 µL with water. The *β-gal* forward and reverse primers amplified a 200 bp fragment from the wild-type allele, whereas the *Neo* forward and reverse primer amplified a 500 bp fragment from the disrupted allele. The DNA was amplified using the following protocol: Initial denaturation 95˚C for 2 min, followed by 35 cycles of denaturation at 94˚C for 1 minute; annealing 63˚C for 1 min; extension at 72˚C for 1 min; and a final extension at 72˚C for 10 min following the last cycle.

Tissue Processing

All mice were sacrificed by cervical dislocation. For neurochemical analysis: optic and sciatic nerves were isolated from each mouse and were immediately frozen on dry ice, then stored at -80^{o}C until ready to use. Nerves were pooled from 11 - 20 mice (22 - 40 nerves) for each sample. Three sets of pooled samples were analyzed for each genotype [wild type (+/+), heterozygous (+/-), knockout (-/-)] and age (7 and 10 months). For XRD analysis: optic and sciatic nerves were bathed with physiological saline (pH 7.4) during dissection,

tied off with surgical silk, and immediately placed in fresh saline, as previously described (Avila *et al.* 2005, Agrawal *et al.* 2009). The nerves were inserted into 0.5 mm and 0.7 mm quartz capillaries (Charles Supper Co., Natick, MA), for optic and sciatic nerves respectfully, which were filled with saline and sealed at both ends with paraffin wax. XRD analysis was performed immediately after dissection, as described below.

Isolation and Purification of Lipids

Complete lipid isolation, purification, and quantitation have been previously described and are as follows (Heinecke *et al.* 2011, Hauser *et al.* 2004, Kasperzyk *et al.* 2004, Seyfried *et al.* 1978).

Total lipid extraction

Lipids were extracted from lyophilized nerve tissue resuspended in 0.5 ml water, with 5 ml chloroform ($CHCl_3$):methanol (CH_3OH) (1:1 by volume). Shaking with a magnetic stirring bar at room temperature overnight dispersed the tissue. The solution was centrifuged and the supernatant was saved. The pellet was washed with 2 ml $CHCl_3$:CH_3OH (1:1 by volume) and the combined supernatants were converted to $CHCl_3$:CH_3OH:dH_2O (30:60:8 by volume).

Column Chromatography/Neutral Lipid Purification

Neutral lipids and acidic lipids were separated using DEAE-Sephadex (A-25, Pharmacia Biotech, Upsala, Sweden) column chromatography, with a 1.2 ml

bed volume (Macala *et al.* 1983, Heinecke *et al.* 2011). The total lipid extract, suspended in solvent A ($CHCl_3$:CH_3OH:water, 30:60:8 by volume), was applied to a DEAE-Sephadex column that had been equilibrated with solvent A. The column was washed twice with solvent A and the entire neutral lipid fraction, consisting of the initial eluent plus washes, was collected. This fraction contained cholesterol, ceramide, phosphatidylcholine, phosphatidylethanolamine and plasmologens, sphingomyelin, cerebrosides and asialo-gangliosides (GA1). Neutral lipids were dried using the EZ-2 evaporator (Genevac, Gardiner, NY) and resuspended in $CHCl_3$:CH_3OH (1:1 by volume). Acidic lipids were eluted from the column with solvent B ($CHCl_3$:CH_3OH:0.8M sodium acetate, 30:60:8 by volume).

Folch Partioning of Acidic Lipids and Gangliosides

The acidic lipids, eluted from the DEAE-Sephadex, were dried by rotary evaporation and resuspended in 7 ml $CHCl_3$: CH_3OH (1:1 by volume). Chloroform (3.5 ml) and water (2.6 ml) were added to the sample to partition gangliosides into the upper phase and acidic phospholipids into the lower phase (Seyfried *et al.* 1978, Folch *et al.* 1957). The upper aqueous phase was removed and the lower organic phase was washed once with 4.5 ml Folch 'pure solvent upper phase' solution ($CHCl_3$:CH_3OH:dH_20, 3:48:47 by volume). The second ganglioside fraction was combined with the first fraction. The acidic phospholipid fraction was evaporated under a stream of nitrogen gas (N_2) and resuspended in $CHCl_3$:CH_3OH (1:1 by volume). This acidic fraction contained cardiolipin, phosphatidylserine, phosphatidylinositol, and sulfatides.

Resorcinol Assay

The amount of sialic acid in the ganglioside fraction was determined by a modified resorcinol assay before and after base treatment and desalting (Svennerholm 1957). NANA (Sigma, St. Louis, MO) was used as a standard curve for total ganglioside analysis. An aliquot of the ganglioside fraction or ganglioside standard was dissolved in 1 ml resorcinol reagent: water (1:1 by volume), boiled for 15 minutes, and cooled in an ice bath. Butyl acetate:1-butanol (1.5 ml) (85:15 by volume) was added and the samples were vortexed and centrifuged for 2 minutes. The supernatant was analyzed in the Shimadzu UV-1601 ultraviolet-visible spectrophotometer (Shimadzu, Kyoto, Japan).

Base Treatment and Desalting

After Folch partitioning, the ganglioside fraction was further purified with base treatment and desalting (Heinecke *et al.* 2011, Hauser *et al.* 2004, Kasperzyk *et al.* 2004). The samples were dried under N_2 and by vacuum lyophilization, then treated with 1ml of 0.15 M sodium hydroxide in a shaking water bath at 37^{o}C for 1.5 hours. Samples were then applied to an equilibrated C18 reverse-phase Bond Elute column (Varian, Harbor City, CA) and washed with water to remove the salts. Gangliosides were eluted from the column with CH_3OH and $CHCl_3$:CH_3OH, evaporated under N_2, and resuspended in $CHCl_3$:CH_3OH (1:1 by volume).

High-performance thin-layer chromatography (HPTLC)

All lipids were analyzed qualitatively by high-performance thin-layer chromatography (HPTLC) (Ando *et al.* 1978, Kasperzyk *et al.* 2004, Macala *et al.* 1983, Seyfried *et al.* 1978). Lipids were spotted on 10 x 20 cm, for gangliosides, or 20 x 20 cm, for neutral and acidic lipids, Silica gel 60 HPTLC plates (E. Meerck, Darmstadt, Germany): 1.5 μg sialic acid for gangliosides, 80 μg nerve dry weight for neutral lipids, and 200 μg nerve dry weight for acidic lipids. To enhance precision, an internal standard (oleyl alcohol) was added to each sample and standard for neutral and acidic lipids, as previously described (Macala *et al.* 1983). Purified lipid standards (Matreya, Inc, Pleasant Gap, PA and Sigma, St. Louis, MO) were spotted on plates at 2, 4 and 8 μg, where the concentration is equivalent to the amount of each lipid per standard lane; except for the GA1 standard, which was spotted at 1, 2 and 4 μg.

For gangliosides, the HPTLC plates were developed with $CHCl_3$: CH_3OH: 0.02% calcium chloride (55:45:10 by volume) and the bands were visualized with resorcinol spray and burning at 100^{o}C for 10 minutes (Kasperzyk *et al.* 2004, Hauser *et al.* 2004)**.** For neutral and acidic phospholipids, the plates were developed with $CHCl_3$: CH_3OH: acetic acid: formic acid: water (35:15:6:2:1 by volume) to a height of either 10 cm or 12 cm, respectively, and then both were developed to the top with hexanes: diisopropyl ether: acetic acid (65:35:2 by volume) (Seyfried *et al.* 1984a, Macala *et al.* 1983). The neutral and acidic lipids

were visualized with 3% copper acetate: 8% phosphoric acid spray and heating at 160^{o}C for 7 minutes.

Densitometry

Individual lipid bands were analyzed by scanning the plates using a Camag TLC scanner 4 (Wilmington, NC), which is controlled by winCATS, Planer Chromatograpy Manager software (Muttenz, Switzerland). The HPTLC plates were placed face up on the scanner sample tray. Deuterium and tungsten-halogen lamps were used to visual bands in the 190-450 nm range and the 350-900 nm range, respectively. Gangliosides were scanned at 580 nm wavelength and neutral and acid lipids were scanned at 328 nm wavelength. Single level calibration mode measured absorption for the evaluation of peak height and area. The total lipid distribution per lane of each plate was normalized to 100% and the percentage distribution values were determined. The percent distribution of total gangliosides was used to calculate sialic acid concentration of individual gangliosides (Seyfried *et al.* 1982, Macala *et al.* 1983). Neutral and acidic lipids were calculated from the standard curve (Macala *et al.* 1983).

X-Ray Diffraction

XRD experiments and analysis were conducted using standard lab protocols, and is illustrated in Figure 10 (Avila *et al.* 2005, Agrawal *et al.* 2009). All diffraction experiments were carried out using nickel-filtered, single-mirror focused Cu Ka radiation from a fine-line source on a 3.0 kW Rigaku x-ray generator (Rigaku/MSC Inc., The Woodlands.TX) operated at 40 kV by 14 to 22

mA. The x-ray diffraction patterns were recorded for 1 hour using a linear, position-sensitive detector (Molecular Metrology, Inc., Northampton, MA), and analyzed using PeakFit (Jandel Scientific, San Rafael, CA). For calculation purposes, the specimen-to-film distance (approximately 200 mm) is expressed as channel number. The integral width of the direct beam in Gaussian form was 7.4 channels (or 8.2 X 10^{-4} $Å^{-1}$).

The positions of the intensity maximizing the diffraction patterns were used to calculate the myelin period (*d*). Background intensity (*B*), approximated as a polynomial curve, was subtracted from the total intensity (*M*+*B*), and the total integral area of the Bragg peaks coming from the myelin (*M*), was obtained. The relative amount of myelin is calculated when the total intensity coming from the multilamellar myelin (*M*, or the peak intensities above background) is divided by the total intensity coming form the volume of nerve subtended by the X-ray beam (*M*+*B*), or [*M*/(*M*+*B*)] (Avila *et al.* 2005).

Statistical Analysis

All XRD values for the *β-gal* +/? and *β-gal* -/- mice were presented as mean ± SD and all neurochemical values for *β-gal* +/? and *β-gal* -/- mice were presented as mean ± SE. All data was analyzed for significance using the two-tailed Student's *t*-Test.

Figure 10. Illustration of X-ray Diffraction. Whole nerves are examined and the x-ray scatter can be recorded on film or an electronic detector. From the x-ray pattern, the myelin period can be measured from the intensity of the Bragg orders. After background subtraction, integrated intensities are used to calculate structure amplitudes and determine the relative amount of myelin, as described in Materials and Methods. Modified from (Avila *et al.* 2005)

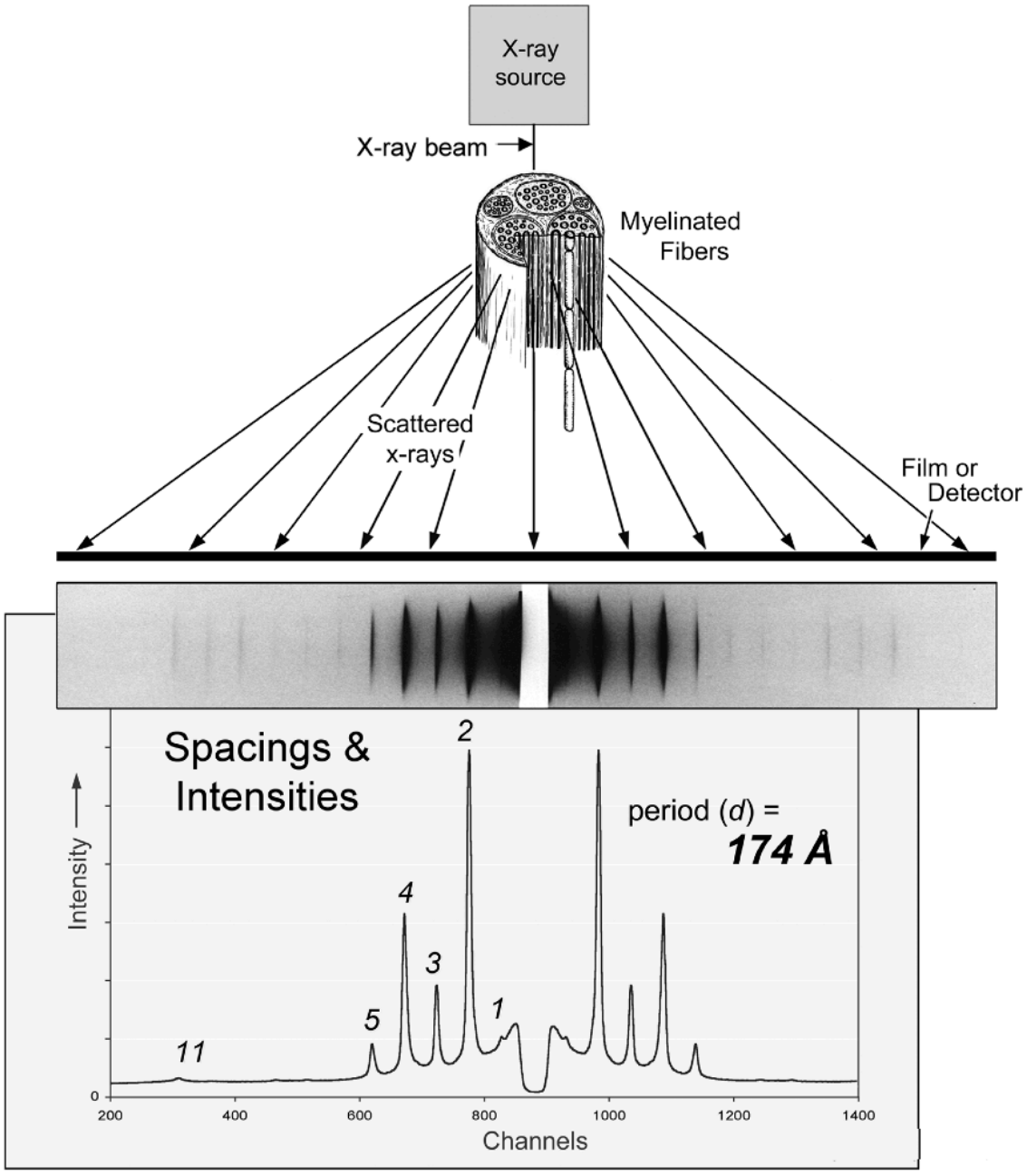
X-ray source
X-ray beam
Myelinated Fibers
Scattered x-rays
Film or Detector
Spacings & Intensities
period (d) =
174 Å
Intensity
Channels
0
200
400
600
800
1000
1200
1400
1
2
3
4
5
11

CHAPTER Three

RESULTS

The objective of this study was to determine if the content and composition of lipids and myelin structure were altered in optic and sciatic nerves in mice with GM1-gangliosidosis. Lipid analysis and XRD were used to analyze the optic and sciatic nerves in mice with GM1-gangliosidosis.

Lipid Analysis

Optic Nerves

The average weight per optic nerve was significantly lower in the *β-gal* -/- mice than in the *β-gal* +/? mice at 7 and 10 month (Table I). The content of total gangliosides and GA1 was significantly greater in optic nerves of the *β-gal* -/- mice than in the *β-gal* +/? mice (Table I and Figure 11). The qualitative and quantitative distributions of the individual ganglioside species in the optic nerves from 7 and 10 month old mice are shown in Table II and Figure 12. Ganglioside GM1 increased in the optic nerves of 7 and 10 month old *β-gal* -/- mice by 50% compared to the *β-gal* +/? mice. There was a corresponding decrease in the more complex gangliosides GT1b and GQ1b in the optic nerves of *β-gal* -/- mice, compared to *β-gal* +/? mice. The gangliosides decreased by 47% (GT1b) and 41% (GQ1b) in 7 month old mice, and by 52% (GT1b) and 54% (GQ1b) in 10 month old mice. Ganglioside GD1a increased 11% in 10 month old *β-gal* -/- compared to the *β-gal* +/? mice.

The qualitative and quantitative distribution of neutral (Figure 11) and acidic (Figure 13) lipids in the optic nerves from 7 and 10 month old mice are shown in Table III. Total cerebrosides were decreased in the optic nerves of *β-gal* -/- mice compared to *β-gal* +/? mice, by 32% at 7 months and 48% at 10 months. Cholesteryl esters increased significantly, whereas there were no significant differences in cholesterol of 7 and 10 month *β-gal* -/- mice compared to *β-gal* +/? mice. Phosphatidylethanolamines were also reduced in *β-gal* -/- mice compared to *β-gal* +/? mice at 10 months. Sulfatides decreased in the optic nerves of *β-gal* -/- mice compared to *β-gal* +/? mice, by 24% at 7 months and 32% at 10 months. Additional acidic lipids, phosphatidic acid, phosphatidylserine, and phosphatidylinositol, increased with some variability between samples but showed no overall differences between the optic nerves of *β-gal* -/- and *β-gal* +/? mice (data not shown). Cardolipin was not detected in optic nerves. The band intensity between the lower and upper bands of cerebrosides and sulfatides were analyzed (Table IV). The doublets observed in cerebroside and sulfatide are due to the presence or absence of hydroxylation at the C1 position (Figure 1), as well as differential FA composition of the fatty acyl chain. No differences were found in the band ratio for cerebrosides or sulfatides in optic nerve.

Sciatic Nerve

There were no significant differences in the weight or lipid content of sciatic nerves between 7 and 10 months of age, so these two groups were combined. No differences were observed in the sciatic nerves of *β-gal* -/- mice in the average weight per nerve, or the content of sialic acid, neutral, or acidic lipids (Figures 11, and 13, and Tables I, III, IV, and data not shown). GA1 was present in the sciatic nerves of *β-gal* -/- mice (Figure 11 and Table I). The qualitative and quantitative distribution of the individual ganglioside species in the sciatic nerves from 7 and 10 month old mice are shown in Figure 12 and Table II. There was a 64% increase in ganglioside GM1 in the sciatic nerves of 7 and 10 month old *β-gal* -/- compared to the *β-gal* +/? mice. The sciatic nerves of *β-gal* -/- mice showed no other differences in ganglioside content.

X-ray Diffraction

Fresh optic and sciatic nerves were dissected from *β-gal* +/? and *β-gal* -/- mice and evaluated by XRD analysis. Membrane packing refers to compaction of the individual opposing surfaces (extracellular / intracellular) of the myelin membrane. Based on the relative strengths of the diffraction patterns, as seen in Figure 14, the relative amounts of myelin were approximately 50% and 10% lower in the optic and sciatic nerves, respectively, of *β-gal* -/- mice, in comparison to *β-gal* +/? mice (Figure 15 and Table V). Myelin periodicity refers to the repeat distance from the pair of membranes, which constitutes the structural unit in the multilamellar sheath. A slight, but significant, reduction was also seen in myelin

periodicity in the optic nerve of *β-gal* -/- mice, compared to *β-gal* +/? mice. XRD analysis revealed no differences in the myelin period in sciatic nerves.

Table I Glycosphingolipid content in optic and sciatic nerves of *β-gal* mice[a]

Nerve Type	Genotype	Age (months)	*N*[b]	Avg. wt/nerve (μg)	μg SA/100 mg dry weight[c]	mg GA1/100 mg dry weight[d]
Optic	+/?	7	5	0.23 ± 0.00	126 ± 4	0.00 ± 0.00
	-/-		3	0.18 ± 0.00 *	162 ± 3 *	1.08 ± 0.08 *
	+/?	10	3	0.28 ± 0.01	144 ± 3	0.00 ± 0.00
	-/-		3	0.15 ± 0.01 *	197 ± 7 *	1.22 ± 0.10 *
Sciatic	+/?	7, 10	8	1.12 ± 0.04	39 ± 6	0.00 ± 0.00
	-/-		6	1.04 ± 0.04	44 ± 6	0.15 ± 0.04 *

[a] Values represent the mean ± SE

[b] *N* = the number of independent samples analyzed, where 22-40 nerves were pooled for each sample.

[c] SA = Sialic Acid, values determinded by resorcinol assay.

[d] Values determined from densitometric scanning of HPTLC plates as shown in Figures 1.

Asterisks indicate that the value is significantly different from that of the control mice at * = $p \leq 0.01$ as determined by the two-tailed t-test.

Figure 11. High-performance thin-layer chromatogram of neutral lipids in the optic and sciatic nerves of *β-gal* -/- and +/? mice. Representative samples for each age group and/or tissue type presented. The amount of total lipids spotted per lane was equivalent to approximately 80 μg nerve dry weight. The plate was developed and the lipid bands visualized as described in the methods section. Std indicates 4 mg of neutral lipid standards and 2 mg of GA1 standard. CE, cholesteryl ester; TG, triglyceride; IS, internal standard (oleoyl alcohol); C, cholesterol; CM, ceramide; CBU, cerebroside upper band; CBL, cerebroside lower band; PE, phosphatidylethanolamine; PC, phosphatidylcholine; SM, sphingomyelin; LPC, lysophosphatidylcholine. SF, indicates the solvent front. The arrows indicate the presence of GA1 in the specific samples. Optic nerve contained no visible TG and sciatic nerves contained no visible CE.

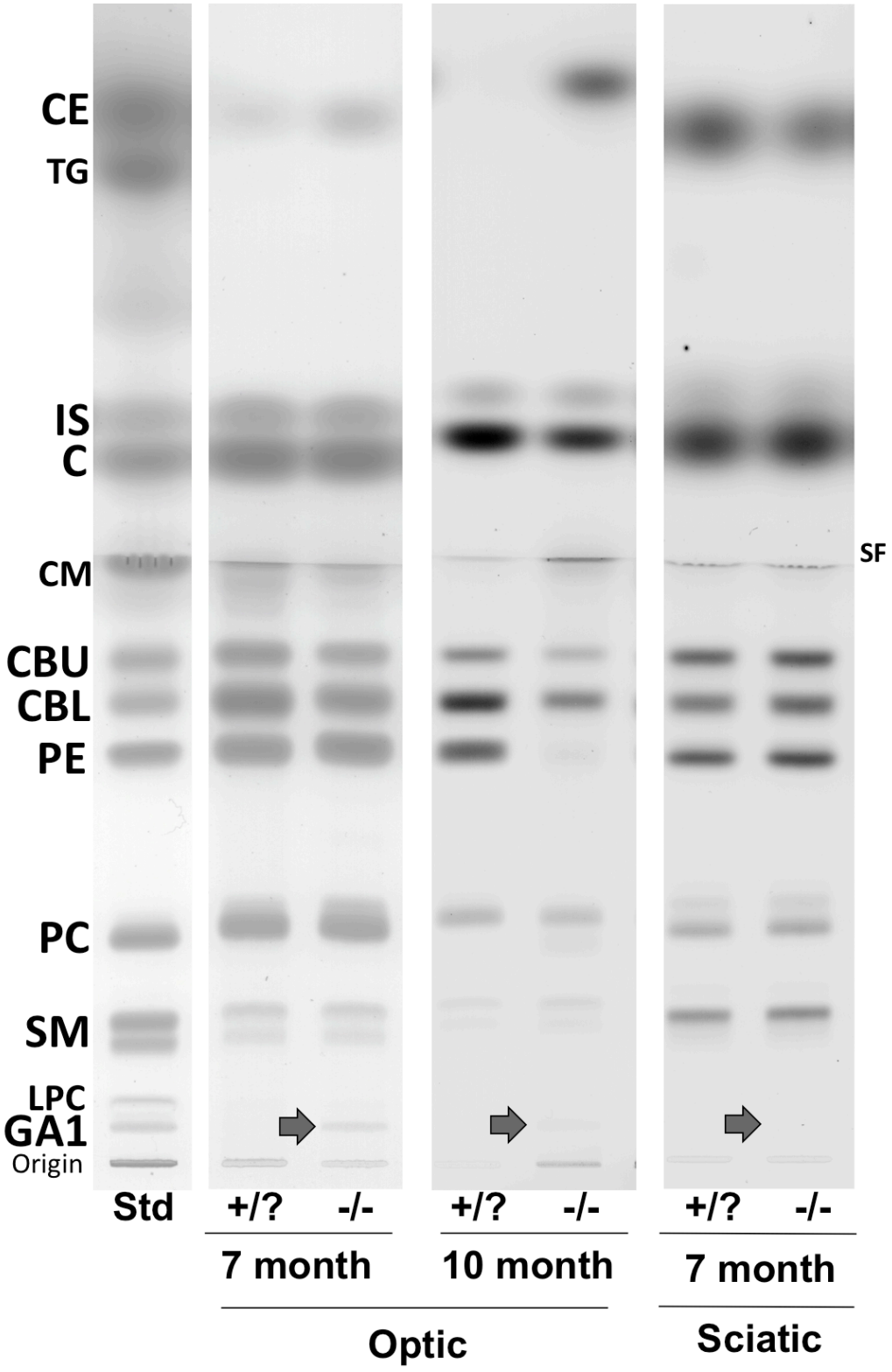
CE
TG
IS
C
CM
CBU
CBL
PE
PC
SM
LPC
GA1
Origin
SF
Std
+/?
-/-
+/?
-/-
+/?
-/-
7 month
10 month
7 month
Optic
Sciatic

Table II Ganglioside distribution in the nerves of *β-gal* mice[a]

Ganglioside (Total content)	Optic Nerve				Sciatic Nerve	
	7 month		10 month		7, 10 months	
	+/?	-/-	+/?	-/-	+/?	-/-
GM1	25.3 ± 0.8	51.5 ± 0.9 *	25.6 ± 1.8	50.9 ± 1.9 *	5.3 ± 0.3	14.6 ± 2.6 *
GD1a	21.8 ± 0.5	19.4 ± 0.6	17.6 ± 0.2	19.8 ± 1.2 *	34.8 ± 0.4	32.5 ± 0.8
GT1a/LD1	3.5 ± 0.2	3.6 ± 0.3	4.3 ± 0.7	2.8 ± 0.2	3.0 ± 0.2	3.0 ± 0.4
GD1b	7.0 ± 0.2	6.1 ± 0.4	10.1 ± 0.3	6.5 ± 0.3	5.2 ± 0.1	5.5 ± 0.4
GT1b	24.7 ± 1.3	13.0 ± 0.6 *	27.6 ± 0.9	13.3 ± 1.3 *	25.3 ± 0.7	21.3 ± 0.8
GQ1b	13.8 ± 0.3	8.2 ± 0.2 *	16.6 ± 0.5	7.6 ± 0.6 *	19.3 ± 0.5	16.1 ± 0.9

[a] Values determined from densitometric scanning of HPTLC plates as shown in Figure 2, are expressed as percent distribution of ganglioside and represent the mean $\pm$SE. The number of independent samples analyzed per nerve type and age group are listed in Table I.

Asterisks indicate that the value is significantly different from that of the control mice at * = $p<0.01$ and as determined by the two-tailed t-test.

Figure 12. High-performance thin-layer chromatogram of gangliosides in the optic and sciatic nerves of *β-gal* -/- and +/? mice. Approximately 1.5 μg ganglioside sialic acid were spotted per lane. Std indicates the ganglioside standards for the labeled gangliosides, gangliosides GM2 and GD3 were not visualized in the nerve lipids. The plate was developed and the lipid bands visualized as described in the methods section.

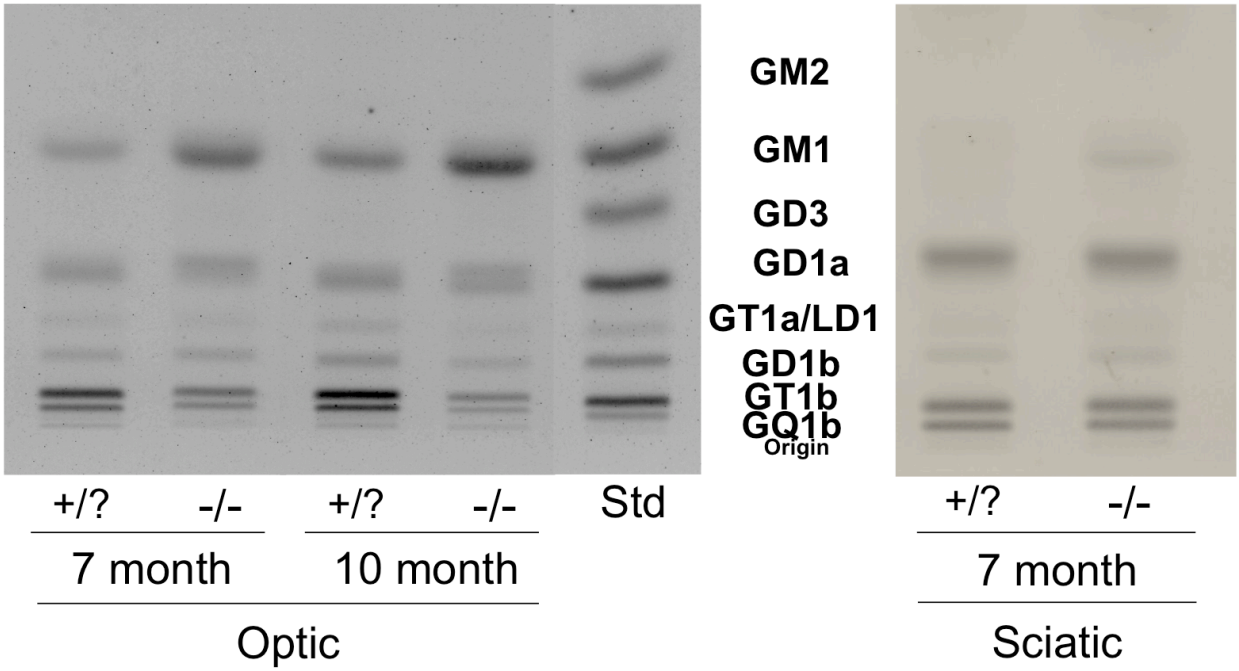
GM2
GM1
GD3
GD1a
GT1a/LD1
GD1b
GT1b
GQ1b
Origin
+/?
-/-
+/?
-/-
Std
7 month
10 month
Optic
+/?
-/-
7 month
Sciatic

Table III Lipid distribution in the optic and sciatic nerves of *β-gal* mice[a]

	Concentration (mg lipid/100 mg dry weight)[b]							
	Optic						Sciatic	
	7 month			10 month			7, 10 month	
Lipids	+/?	-/-		+/?	-/-		+/?	-/-
Neutral								
Cholesterol Ester	1.3 ± 0.1	2.2 ± 0.1	*	0.6 ± 0.1	6.5 ± 0.3	**	ND	ND
Triacylglycerol	ND	ND		ND	ND		6.8 ± 0.7	6.8 ± 1.3
Cholesterol	10.0 ± 0.2	10.1 ± 0.4		11.1 ± 0.9	10.4 ± 0.9		7.0 ± 0.7	7.2 ± 1.0
Cerebrosides	12.0 ± 0.4	8.2 ± 0.4	**	11.4 ± 0.1	5.9 ± 0.2	**	6.4 ± 0.5	7.2 ± 1.0
Phosphatidylethanolamine	11.1 ± 0.7	10.4 ± 0.5		8.6 ± 0.4	1.2 ± 0.1	**	5.3 ± 0.4	6.0 ± 0.5
Phosphatidylcholine	7.2 ± 0.3	7.1 ± 0.1		5.8 ± 0.4	5.5 ± 0.6		3.4 ± 0.2	3.9 ± 0.3
Sphingomyelin	1.6 ± 0.1	1.8 ± 0.1		1.2 ± 0.1	1.1 ± 1.3		2.9 ± 0.3	3.4 ± 0.6
Acidics								
Sulfatides	3.7 ± 0.1	2.8 ± 0.2	*	3.8 ± 0.1	2.6 ± 0.1	**	1.8 ± 0.1	1.6 ± 0.2

[a] Values determined from densitometric scanning of HPTLC plates, as shown in Figures 1 & 3, and represent the mean ± SE. The number of independent samples analyzed per nerve type/age group are listed in Table I.

[b] Values are expressed as mg of each lipid/100 mg dry weight of the total sample. The asterisks indicate that the value is significantly different from that of the control mice at * = $p<0.02$ and ** = $p<0.001$, as determined by the two-tailed t-test.

Figure 13. High-performance thin-layer chromatogram of acidic lipids in the optic and sciatic nerves of *β-gal* -/- and +/? mice. Representative samples for each age group and/or tissue type presented. The amount of total lipids spotted per lane was equivalent to approximately 200 μg nerve dry weight for the acidic lipids. The plate was developed and the lipid bands visualized as described in the methods section. Std indicates 4 mg acidic lipid standards. IS, internal standard (oleoyl alcohol); CL, cardiolipin; PA, phosphatidic acid; SFU, sulfatide upper band; SFL, sulfatide lower band; PS, phosphatidylserine; PI, phosphatidylinositol. SF, indicates the solvent front.

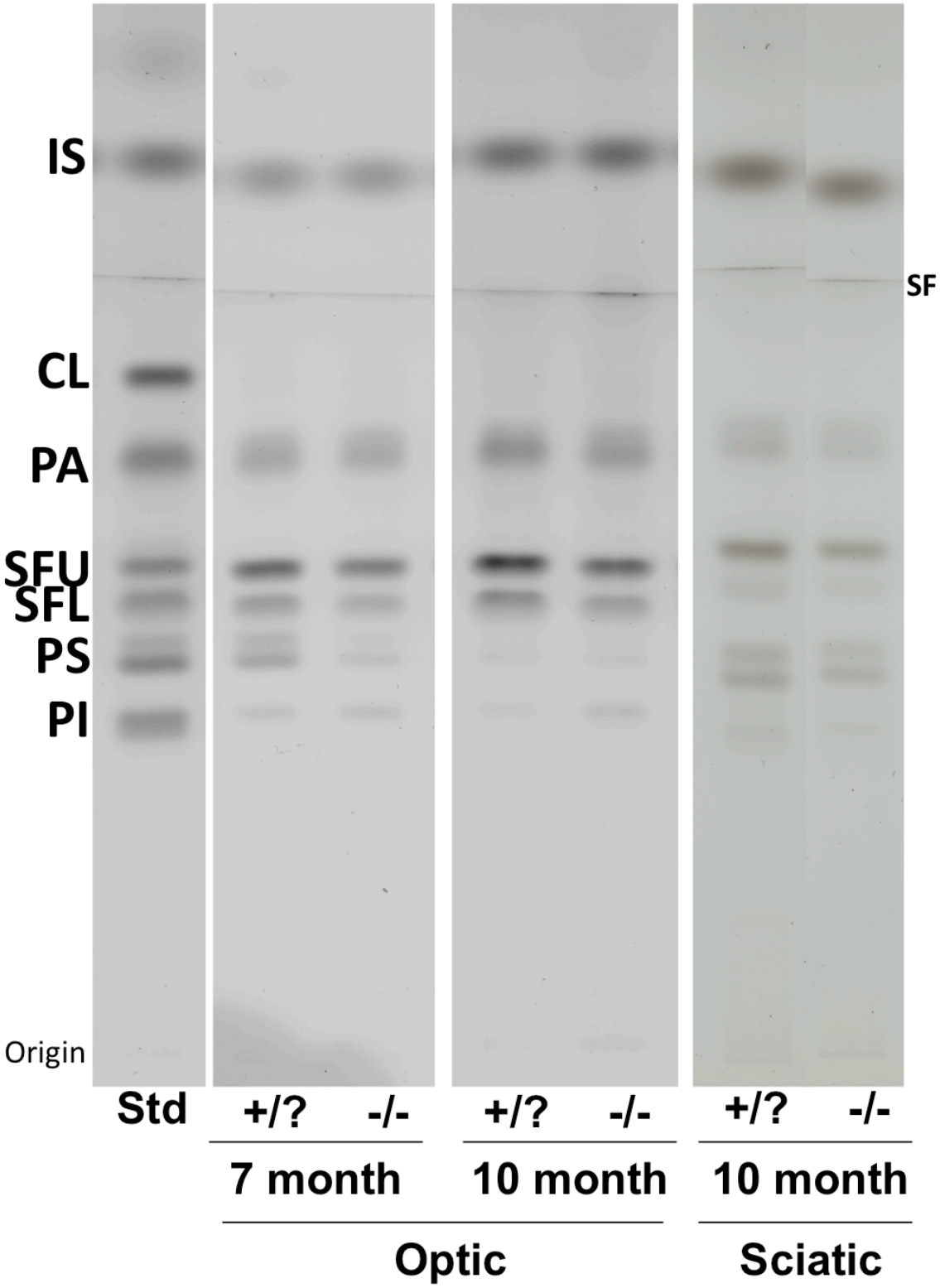
IS
SF
CL
PA
SFU
SFL
PS
PI
Origin
Std
+/?
-/-
+/?
-/-
+/?
-/-
7 month
10 month
10 month
Optic
Sciatic

Table IV Upper and lower band content in cerebrosidse and sulfatides of *β-gal* nerves[a]

			Cerebrosides[b]			Sulfatides[b]		
Nerve Type	Genotype	Age (months)	Lower	Upper	L/U[c] Ratio	Lower	Upper	L/U[c] Ratio
Optic	+/?	7	63.1	37.0	1.71 ± 0.02	31.9	68.1	0.47 ± 0.01
	-/-		64.4	35.6	1.81 ± 0.02	33.1	66.9	0.49 ± 0.01
	+/?	10	65.5	34.5	1.90 ± 0.01	33.6	66.4	0.51 ± 0.01
	-/-		70.3	29.7	2.38 ± 0.16	37.9	62.1	0.61 ± 0.03
Sciatic	+/?	7,10	50.3	49.7	1.01 ± 0.01	26.9	73.0	0.37 ± 0.01
	-/-		50.4	49.6	1.02 ± 0.01	26.7	73.3	0.37 ± 0.02

[a] Values determined from densitometric scanning of HPTLC plates, as shown in Figures 1 (cerebrosides) & Figure 3 (sulfatides), and represent the mean (for individual bands) or mean ± SE (for the band ratio).The number of independent samples analyzed per nerve type and age group are listed in Table I

[b] Values represent the percentage of total cerebroside or sulfatide in the lower or upper band of each lipid.

[c] L/U represents the ratio of the lower band to the upper band.

Table V X-Ray diffraction analysis of *β-gal* mice[a]

	Optic Nerve		Sciatic Nerve	
	+/?	-/-	+/?	-/-
Age (days)	207 ± 15	210 ± 20	207 ± 15	210 ± 20
M/(M+B)[b]	0.245 ± 0.01	0.120 ± 0.02 **	0.368 ± 0.02	0.324 ± 0.05 *
d[c]	156.2 ± 0.4	155.3 ± 0.5 **	175.4 ± 0.5	176.0 ± 1.0

[a] Values represent mean±SD. *N* = 12 nerves per group for *β-gal* +/?, and 6 nerves per group for *β-gal* -/-. Optic and Sciatic nerves were from the same mice.

[b] M/(M+B) = The myelin content of fresh nerves, based on the ratio of the X-ray diffraction scatter of the peaks over the total scatter, as shown in Figure 4.

[c] d = the periodicity of the peaks, as shown in Figure 2, and is displayed as angstroms (Å).

Astericks indicate statistical significance where * = $p<0.03$ and ** = $p<0.001$, based on Student's two tailed t-test

Figure 14. X-ray diffraction from optic and sciatic nerves of *β-gal* mice. Representative examples of data for optic (left) and sciatic (right) nerves from *β-gal* +/? and *β-gal* -/- are shown. Myelin scatter was significantly weaker in optic nerves ($p < 0.001$) and in sciatic nerves ($p < 0.03$) of *β-gal* -/- mice than in *β-gal* +/? mice. The Bragg orders for the x-ray peaks are indicated 2-5.

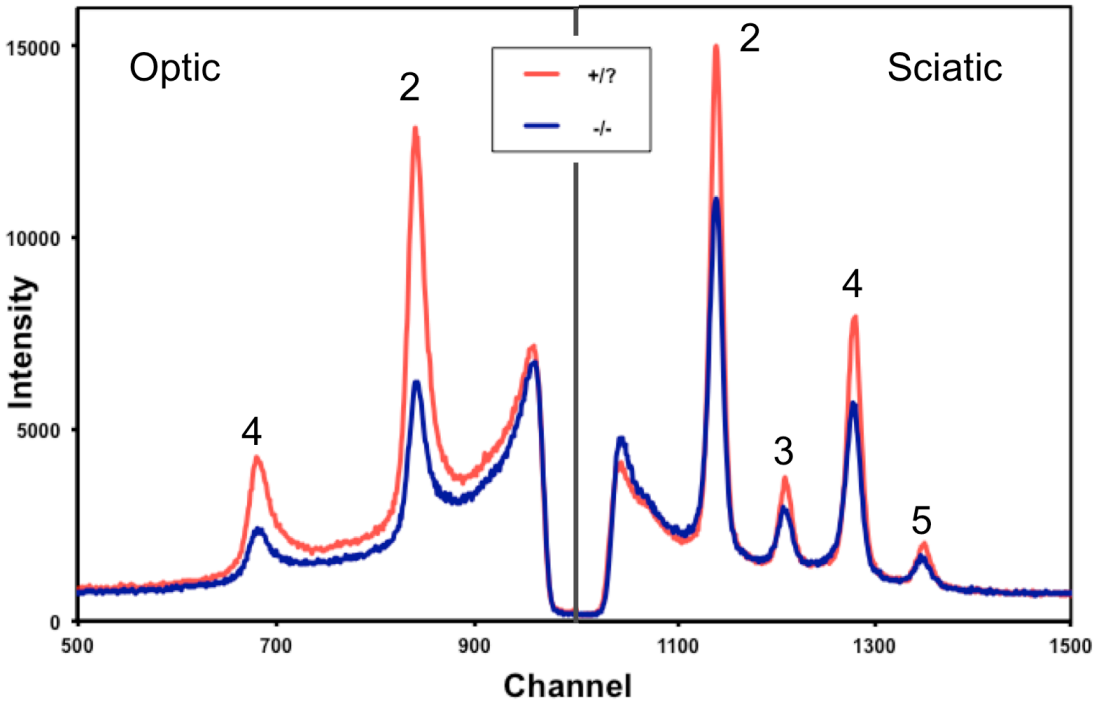
Optic
Sciatic
+/?
-/-
2
2
4
4
3
5
15000
10000
5000
0
Intensity
500
700
900
1100
1300
1500
Channel

Figure 15. XRD analysis of myelin content and myelin periodicity of *β-gal* -/- and *β-gal* +/? mice. The fractional amount of scatter by compact myelin (M) compared to the relative amount of total x-ray scatter (M+B) is plotted against the myelin period, in Angstroms (Å). The mean value and standard deviations are indicated for each group of data (*N* = 12 nerves per group for *β-gal* +/?, and 6 nerves per group for *β-gal* -/-). The relative amount of myelin was significantly lower in the optic and sciatic nerves of *β-gal* -/- (circles) mice compared to *β-gal* +/? (diamonds) mice. Myelin periodicity was significantly less in the optic nerves of *β-gal* -/- (circles) mice than in *β-gal* +/? (diamonds) mice. The sciatic nerves of *β-gal* -/- (circles) and *β-gal* +/? (diamonds) mice showed no significant differences in periodicity. Asterisks indicate statistical significance of $p < 0.003$, based on Student's two-tailed unpaired *t*-test.

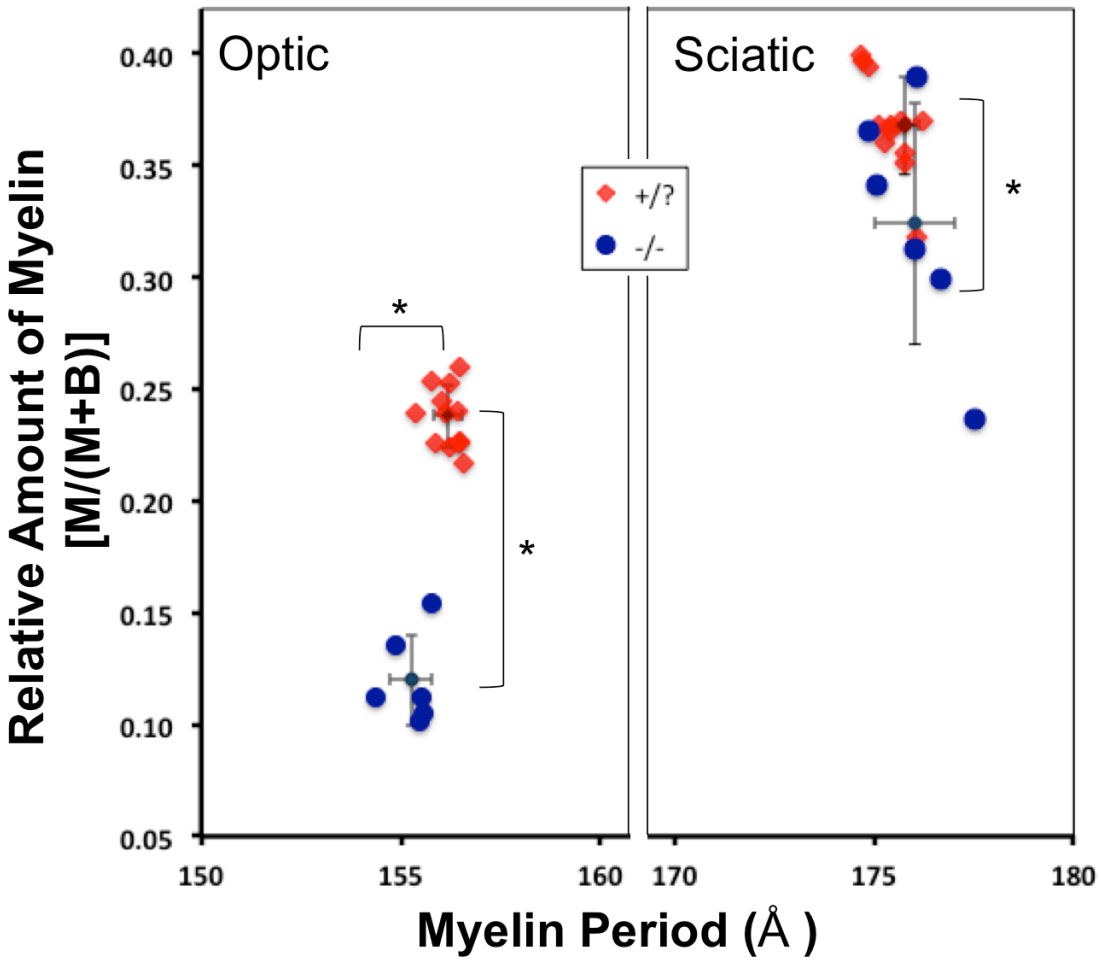
Optic
Sciatic
+/?
-/-
*
*
*
Relative Amount of Myelin
[M/(M+B)]
0.40
0.35
0.30
0.25
0.20
0.15
0.10
0.05
150
155
160
170
175
180
Myelin Period (Å)

CHAPTER FOUR

DISCUSSION

In whole brain analysis, mice with GM1-gangliosidosis have reduced brain weights, and an increase in total ganglioside content, GM1, and GA1 (Vajn *et al.* 2013, Yu *et al.* 1975, Baek *et al.* 2010, Hahn *et al.* 1997, Matsuda *et al.* 1997b, Broekman *et al.* 2007, Kasperzyk *et al.* 2005). The optic nerves also had a significant reduction in weight per nerve and a reduction in the amount of myelin per nerve. This reduction per nerve, in addition to reduction in the amount of nerves in GM1-ganliosidosis brains, could affect the total brain weight reduction previously seen in diseased brain (Tessitore *et al.* 2004, van der Voorn *et al.* 2005). Ganglioside content has been shown to increase in myelin with age, and the same trend was observed in the optic nerves of *β-gal* +/? mice between 7 and 10 months of age (Suzuki *et al.* 1967, Yu *et al.* 1975). The increase in ganglioside content was even greater among *β-gal* -/- mice compared to controls, due to the increase in GM1 content, as previously seen in whole brains (Broekman *et al.* 2007, Kasperzyk *et al.* 2005, Baek *et al.* 2010).

Enrichment of ganglioside GM1 and GA1 was observed in the optic and sciatic nerves of *β-gal* -/- mice. Control nerves exhibit the ganglioside pattern that is normally observed in adult and aging brains (Seyfried *et al.* 2009, Heinecke *et al.* 2011, Broekman *et al.* 2007, Baek *et al.* 2010, Yu *et al.* 1975). These data

suggest that GM1 and GA1 accumulation in the brains of *β-gal* -/- mice are also observed in the optic and sciatic nerves. Nevertheless, the optic nerves of *β-gal* -/- mice had additional ganglioside abnormalities not previously observed in the whole brain; specifically, reduction of GT1b and GQ1b and an increase in GD1a. However, while not consistent in all brain regions (cortex, cerebellum, brainstem, and spinal cord) or statistically significant, Baek *et al.* 2010 did observe reduction in GT1b and GQ1b and an increase in GD1a of *β-gal* -/- mice compared to controls. Since GT1b and GD1a are known to reside in the plasma membrane of axons and contribute to axonal-myelin stability, these lipids might be expected to either increase or decrease concurrently (Vyas *et al.* 2002, Jackman *et al.* 2009). However, the reduction of GT1b and increase of GD1a suggests that their interaction with the axonal plasma membrane occurs independent of each other. The increase in GD1a may occur to compensate for the decrease in GT1b, in an attempt to maintain axonal-myelin integrity. The N-metyl-D-aspartate (NMDA) receptor is the primary pathway for calcium influx into the myelin of optic nerve and is associated with neurotoxicity when activated (Sucher *et al.* 1991, Shin *et al.* 2014, Micu *et al.* 2006). NMDA receptor has also been associated with neurotoxicity in retinal ganglion cell cultures (Sucher *et al.* 1991). GQ1b has been shown to regulate expression of the NMDA receptor protein, and reduction in GQ1b may reduce calcium influx and thus reduce potential neuronal damage (Shin *et al.* 2014, Micu *et al.* 2006).

In addition to ganglioside and weight abnormalities in whole brain of *β-gal* -/- mice, cerebroside and sulfatide content were less in *β-gal* -/- mice then in *β-gal* +/? mice (Matsuda *et al.* 1997a, Baek *et al.* 2010, Hahn *et al.* 1997, Matsuda *et al.* 1997b, Broekman *et al.* 2007, Kasperzyk *et al.* 2005). Cerebrosides and sulfatides are neutral and acidic lipids, respectively, that are enriched in myelin membranes. The cerebroside and sulfatide content was reduced in the optic nerves of *β-gal* -/- mice, corresponding to previously observed reduction in the lipids of whole brain *β-gal* -/- mice. In addition, there was reduction of phosphatidylethanolamine, at 10 months, and an increase in cholesteryl ester at 7 and 10 months in the optic nerves of *β-gal* -/- mice, corresponding to lipid changes seen in humans (Kasama *et al.* 1986, Suzuki *et al.* 1968b). An increase in cholesteryl esters correlates to an increase in inflammation and myelin breakdown in nervous tissue (Yu *et al.* 1982, Mutka *et al.* 2010, Paintlia *et al.* 2003). The majority of phosphatidylethanolamine in myelin is in the form of plasmalogen ethanolamines (Farooqui *et al.* 2001). All ethanolamine lipids are resolved together with TLC analysis, so it was deduced that the reduction in the phosphatidylethanolamine band was a result of a primary reduction in plasmalogen ethanolamines. Reduction in cerebroside, sulfatide, and plasmalogen ethanolamines are known to affect stability in the paranodal junction and the interaction of the paranodal myelin with the axon (Farooqui *et al.* 2001, Chrast *et al.* 2011, Hayashi *et al.* 2013, Marcus *et al.* 2006, Coetzee *et al.* 1996, Viader *et al.* , Ishibashi *et al.* 2002, Jackman *et al.* 2009). This affect at the paranodal junction leads to a reduction in conduction velocity in nerves (Hayashi

et al. 2013, Coetzee *et al.* 1996). These data suggest that the optic nerve lipids were altered in ways that reduce myelin integrity. A reduction in myelin stability and conduction velocity could explain one aspect of the neuronal and visual abnormalities observed in GM1-gangliosidosis mice (Baek *et al.* 2010, Denny *et al.* 2007, Murray *et al.* 1977, Bieber *et al.* 1986).

Cerebrosides and sulfatides appear as double bands on HPTLC plates. The double bands separate based on the amount of hFA and, to a lesser extent, their fatty acyl carbon chain length; where non-hydroxylated molecules run faster, indicated as upper bands, than hydroxylated molecules, indicated as lower bands (Das *et al.* 1978, Karthigasan *et al.* 1996, Ganser *et al.* 1988, Clausen *et al.* 1970, Inouye *et al.* 1985, Blass 1970). The FA content of cerebrosides and sulfatides are mostly hydroxylated, saturated, and longer chain lengths (C22-24), while most phospholipids and gangliosides are non-hydroxylated and shorter chain lengths (C18) (Bosio *et al.* 1998, O'Brien *et al.* 1967, Blass 1970, Menkes *et al.* 1966, Hama). The amounts of upper and lower band lipids in cerebrosides and sulfatides agrees with previous assessment of the FA content of cerebrosides and sulfatides in human white matter and do not appear to be altered in *β-gal* -/- mice nerves (Svennerholm *et al.* 1968, Menkes *et al.* 1966, Horrocks 1973).

The nerves of the PNS are known to be sites of accumulation in some LSD (e.g. GM2-gangliosidosis) (Shapiro *et al.* 2008, Jain *et al.* 2010, Tatematsu

et al. 1981). However, this accumulation of material has not been shown in the peripheral nerves in GM1-gangliosidosis mice, and lipid analysis has not been performed on any peripheral nerves in animals with GM1-gangliosidosis. Yamano *et al.*, showed accumulation of storage material in a human fetus with GM1-gangliosidosis beginning in the PNS, before accumulating in the spinal cord and brain (Yamano *et al.* 1983). The increase of GM1 and GA1 in the sciatic nerves corresponds to the increase of GM1 and GA1 in the optic nerves. However, the additional lipid abnormalities in the optic nerves, compared to whole brain, were not observed in the sciatic nerves. These data suggest that the previously observed accumulation of GM1 and GA1 in the periphery of humans is also observed in the sciatic nerves of *β-gal* -/- mice (Iwamasa *et al.* 1987, Folkerth *et al.* 2000, Nada *et al.* 2011, Suzuki *et al.* 1968b, NINDS 2011).

XRD has been a useful technique in assessing the quantity and compaction of myelin about the nerve (Mateu *et al.* 1991, Kirschner *et al.* 1976, Avila *et al.* 2010, Yin *et al.* 2006, Inouye *et al.* 1985, Karthigasan *et al.* 1996, Kirschner *et al.* 2010, Chia *et al.* 1984, Avila *et al.* 2005, Agrawal *et al.* 2009). The present analysis of *β-gal* +/? nerves are in agreement with previously published data on XRD of other mouse nerves: specifically the amount of myelin and the periodicity of the peaks, in both optic and sciatic nerves (Avila *et al.* 2010, Mateu *et al.* 1991, Agrawal *et al.* 2009). This is the first time XRD analysis has been performed on the nerves in GM1-gangliosidosis animals. These results

correlate with the lipid data, by demonstrating abnormalities to a greater extent in the optic nerve and to a lesser extent in the sciatic nerve.

Humans, mice and other animals with GM1-gangliosidosis, present with retinal and visual abnormalities (Read *et al.* 1976, Suzuki *et al.* 2001, NINDS 2011, Denny *et al.* 2007, Baek *et al.* 2010, Sheahan *et al.* 1978, Murray *et al.* 1977). These abnormalities are characterized by ganglioside accumulation in the retinal ganglion cells and altered myelination of the optic nerve (Muller *et al.* 2001, Brunetti-Pierri *et al.* 2008, Gururaj *et al.* 2005, Di Rocco *et al.* 2005, Shen *et al.* 1998, Kaye *et al.* 1992, Folkerth *et al.* 2000, Sheahan *et al.* 1978). In humans with GM1-gangliosidosis, the retinal ganglion cells have been observed as one of the primary locations for ganglioside accumulation (Weiss *et al.* 1973, Emery *et al.* 1971, Cogan *et al.* 1984, Bieber *et al.* 1986). These abnormalities contribute to blindness as one of the pathological features of GM1-gangliosidosis (Baker *et al.* 1974, Matsuda *et al.* 1997a, Suzuki *et al.* 2001, Baek *et al.* 2010, Hahn *et al.* 1997, Matsuda *et al.* 1997b, Tessitore *et al.* 2004). Baek *et al*., used AAV (adeno-associated virus) vector thalamic gene delivery to correct storage in GM1-gangliosidosis mice (Baek *et al.* 2010). They observed a significant reduction of GM1 and GA1 accumulation in most CNS structures and an increase in survival, but motor abnormalities and blindness were not completely corrected (Baek *et al.* 2010). It has been determined that gangliosides do not move from the retina to the optic nerve (Holm *et al.* 1974, Holm 1972). These data, along with previous studies on the ocular pathway, suggest that alterations

to the retina and optic nerve work in conjunction with the brain to produce visual abnormalities observed in GM1-gangliosidosis.

The structural integrity of the myelin membrane and its interaction with the axon is dependent on the balance of proteins and lipids (FA chain length, saturation, and the lipids present) (Viader *et al.* 2013, Marcus *et al.* 2006, Vyas *et al.* 2002, Jackman *et al.* 2009, Ishibashi *et al.* 2002, Hama 2010). Many lipids act as messengers to stimulate calcium influx, inflammation, apoptosis, etc (Farooqui *et al.* 2001, Kolesnick *et al.* 1999, Platt *et al.* 2012). Changes in lipid content or composition could disrupt the stability and integrity of the myelin membrane. GM1, cholesterol, cerebroside, sulfatide, and plasmalogen ethanolamine are all known to affect stability at the paranodal junction (Farooqui *et al.* 2001, Chrast *et al.* 2011, Hayashi *et al.* 2013, Marcus *et al.* 2006, Coetzee *et al.* 1996, Viader *et al.* , Ishibashi *et al.* 2002, Jackman *et al.* 2009, Susuki *et al.* 2007). Alterations to any of these lipids would compromise the myelin integrity. We observed significant changes in cerebroside, sulfatide, and phosphatidylethanolamine in the optic nerve, and the lipid abnormalities could lead to ER distress, apoptosis, and compromised myelin structure.

To our knowledge this is the first study demonstrating a reduction in the quantity and quality of myelin in the optic and sciatic nerves of mice with GM1-gangliosidosis. Through the combined results of lipid analysis and XRD we were able to correlate our results on control nerves to previous results on white matter

and CNS and PNS nerves. Both analytical techniques have been utilized in the study of myelin stability. The neurochemical pathology was altered in the optic and sciatic nerves of mice with GM1-gangliosidosis. Nerve weight, total gangliosides, GM1, GA1, cerebrosides and sulfatides were altered not just in the brains, but also in the individual nerves of the CNS. Combined with alterations in GD1a, GT1b, GQ1b, cholesteryl ester and plasmalogen ethanolamine (represented by phosphatidylethanolamine) content, these lipid differences resulted in a reduction in the amount of myelin and myelin periodicity in the optic nerves. While PNS involvement was not as drastic as in the CNS, the sciatic nerves did accumulate GM1 and GA1, and they had a reduction in myelin content. Future therapeutic research should analyze optic and sciatic nerves as part of a comprehensive corrective therapeutic regimen.

APPENDIX

Publications

Arthur JA, **Heinecke KA**, Seyfried TN. Filipin recognizes both GM1 and cholesterol in GM1 gangliosidosis mouse brain. J Lipid Res. 52(7):1345-51, 2011

Heinecke KA, Peacock BN, Blazar BR, Tolar J, Seyfried TN. Lipid Composition of Whole Brain and Cerebellum in Hurler Syndrome (MPS IH) Mice. Neurochem Res. 36:1669-1676, 2011

Denny CA, **Heinecke KA**, Kim YP, Baek RC, Loh KS, Butters TD, Bronson RT, Platt FM, and Seyfried TN. Restricted ketogenic diet enhances the therapeutic action of N-butyldeoxynojirimycin towards brain GM2 accumulation in adult Sandhoff disease mice. J Neurochem. 113(6):1525-35, 2010

Seyfried TN, **Heinecke KA**, Mantis JG, and Denny CA. Brain lipid analysis in mice with Rett syndrome. Neurochem Res. 34(6):1057-65, 2009

REFERENCES

AGRAWAL, D., HAWK, R., AVILA, R. L., INOUYE, H. AND KIRSCHNER, D. A. (2009) INTERNODAL MYELINATION DURING DEVELOPMENT QUANTITATED USING X-RAY DIFFRACTION. *J STRUCT BIOL,* 168, 521-526.

ANCHISI, L., DESSI, S., PANI, A. AND MANDAS, A. (2013) CHOLESTEROL HOMEOSTASIS: A KEY TO PREVENT OR SLOW DOWN NEURODEGENERATION. *FRONT PHYSIOL,* 3, 486.

ANDO, S., CHANG, N. C. AND YU, R. K. (1978) HIGH-PERFORMANCE THIN-LAYER CHROMATOGRAPHY AND DENSITOMETRIC DETERMINATION OF BRAIN GANGLIOSIDE COMPOSITIONS OF SEVERAL SPECIES. *ANAL BIOCHEM,* 89, 437-450.

ANDO, S. AND YU, R. K. (1984) FATTY ACID AND LONG-CHAIN BASE COMPOSITION OF GANGLIOSIDES ISOLATED FROM ADULT HUMAN BRAIN. *J NEUROSCI RES,* 12, 205-211.

APPELDOORN, B. J., CHANDROSS, R. J., BEAR, R. S. AND HOGAN, E. L. (1975) AN X-RAY DIFFRACTION STUDY OF CENTRAL AND PERIPHERAL MYELINATION IN JIMPY AND QUAKING MICE. *BRAIN RES,* 85, 517-521.

ASBURY, A. K. (1975) THE BIOLOGY OF SCHWANN CELLS. IN: *PERIPHERAL NEUROPATHY*, (P. J. DYCK, P. K. THOMAS AND E. H. LAMBERT EDS.)*,* PP. 203. W. B. SAUNDERS COMPANY, PHILADELPHIA, LONDON, TORONTO.

AVILA, R. L., D'ANTONIO, M., BACHI, A., INOUYE, H., FELTRI, M. L., WRABETZ, L. AND KIRSCHNER, D. A. (2010) P0 (PROTEIN ZERO) MUTATION S34C UNDERLIES INSTABILITY OF INTERNODAL MYELIN IN S63C MICE. *J BIOL CHEM,* 285, 42001-42012.

AVILA, R. L., INOUYE, H., BAEK, R. C., YIN, X., TRAPP, B. D., FELTRI, M. L., WRABETZ, L. AND KIRSCHNER, D. A. (2005) STRUCTURE AND STABILITY OF INTERNODAL MYELIN IN MOUSE MODELS OF HEREDITARY NEUROPATHY. *J NEUROPATHOL EXP NEUROL,* 64, 976-990.

BAEK, R. C., BROEKMAN, M. L., LEROY, S. G., TIERNEY, L. A., SANDBERG, M. A., D'AZZO, A., SEYFRIED, T. N. AND SENA-ESTEVES, M. (2010) AAV-MEDIATED GENE DELIVERY IN ADULT GM1-GANGLIOSIDOSIS MICE

CORRECTS LYSOSOMAL STORAGE IN CNS AND IMPROVES SURVIVAL. *PLOS ONE,* 5, E13468.

BAKER, H. J. AND LINDSEY, J. R. (1974) ANIMAL MODEL: FELINE GM1 GANGLIOSIDOSIS. *AM J PATHOL,* 74, 649-652.

BAKER, H. J., MOLE, J. A., LINDSEY, J. R. AND CREEL, R. M. (1976) ANIMAL MODELS OF HUMAN GANGLIOSIDE STORAGE DISEASES. *FED PROC,* 35, 1193-1201.

BIEBER, F. R., MORTIMER, G., KOLODNY, E. H. AND DRISCOLL, S. G. (1986) PATHOLOGIC FINDINGS IN FETAL GM1 GANGLIOSIDOSIS. *ARCH NEUROL,* 43, 736-738.

BIEBERICH, E. AND YU, R. K. (1999) MULTI-ENZYME KINETIC ANALYSIS OF GLYCOLIPID BIOSYNTHESIS. *BIOCHIM BIOPHYS ACTA,* 1432, 113-124.

BISEL, B., PAVONE, F. AND CALAMAI, M. (2014) GM1 AND GM2 GANGLIOSIDES: RECENT DEVELOPMENTS. *BIOMOLECULAR CONCEPTS,* 5, 87-93.

BLASS, J. P. (1970) FATTY ACID COMPOSITION OF CEREBROSIDES IN MICROSOMES AND MYELIN OF MOUSE BRAIN. *J NEUROCHEM,* 17, 545-549.

BLAUROCK, A. E., GENTER ST CLAIR, M. B. AND GRAHAM, D. G. (1991) MEMBRANE FLOW WITHIN THE MYELIN SHEATH IN IDPN NEUROPATHY. *NEUROPATHOL APPL NEUROBIOL,* 17, 309-321.

BOSIO, A., BINCZEK, E., HAUPT, W. F. AND STOFFEL, W. (1998) COMPOSITION AND BIOPHYSICAL PROPERTIES OF MYELIN LIPID DEFINE THE NEUROLOGICAL DEFECTS IN GALACTOCEREBROSIDE- AND SULFATIDE-DEFICIENT MICE. *J NEUROCHEM,* 70, 308-315.

BOUKHRIS, A., SCHULE, R., LOUREIRO, J. L. *ET AL.* (2013) ALTERATION OF GANGLIOSIDE BIOSYNTHESIS RESPONSIBLE FOR COMPLEX HEREDITARY SPASTIC PARAPLEGIA. *AM J HUM GENET,* 93, 118-123.

BROEKMAN, M. L., BAEK, R. C., COMER, L. A., FERNANDEZ, J. L., SEYFRIED, T. N. AND SENA-ESTEVES, M. (2007) COMPLETE CORRECTION OF ENZYMATIC DEFICIENCY AND NEUROCHEMISTRY IN THE GM1-GANGLIOSIDOSIS MOUSE BRAIN BY NEONATAL ADENO-ASSOCIATED VIRUS-MEDIATED GENE DELIVERY. *MOL THER,* 15, 30-37.

BROWN, F. R., 3RD, BECK, J. C., NIEBYL, J. R. AND SINGH, I. (1985) EFFECT OF PROTEOLIPID PROTEIN ON CENTRAL NERVOUS SYSTEM MYELIN MEMBRANE FLUIDITY. *NEUROSCI LETT,* 59, 149-154.

BRUNETTI-PIERRI, N., BHATTACHARJEE, M. B., WANG, Z. J., ZILI, C., WENGER, D. A., POTOCKI, L., HUNTER, J. AND SCAGLIA, F. (2008) BRAIN PROTON MAGNETIC RESONANCE SPECTROSCOPY AND NEUROMUSCULAR PATHOLOGY IN A PATIENT WITH GM1 GANGLIOSIDOSIS. *J CHILD NEUROL,* 23, 73-78.

CAIRNS, L. J., GREEN, W. R. AND SINGER, H. S. (1984) GM1 GANGLIOSIDOSIS, TYPE 2: OCULAR CLINICOPATHOLOGIC CORRELATION. *GRAEFES ARCH CLIN EXP OPHTHALMOL,* 222, 51-62.

CHIA, L. S., THOMPSON, J. E. AND MOSCARELLO, M. A. (1984) ALTERATION OF LIPID-PHASE BEHAVIOR IN MULTIPLE SCLEROSIS MYELIN REVEALED BY WIDE-ANGLE X-RAY DIFFRACTION. *PROC NATL ACAD SCI U S A,* 81, 1871-1874.

CHIAVEGATTO, S., SUN, J., NELSON, R. J. AND SCHNAAR, R. L. (2000) A FUNCTIONAL ROLE FOR COMPLEX GANGLIOSIDES: MOTOR DEFICITS IN GM2/GD2 SYNTHASE KNOCKOUT MICE. *EXP NEUROL,* 166, 227-234.

CHOU, D. K., FLORES, S. AND JUNGALWALA, F. B. (1990) LOSS OF SULFOGLUCURONYL AND OTHER NEOLACTOGLYCOLIPIDS IN PURKINJE CELL ABNORMALITY MURINE MUTANTS. *J NEUROCHEM,* 54, 1589-1597.

CHRAST, R., SAHER, G., NAVE, K. A. AND VERHEIJEN, M. H. (2011) LIPID METABOLISM IN MYELINATING GLIAL CELLS: LESSONS FROM HUMAN INHERITED DISORDERS AND MOUSE MODELS. *J LIPID RES,* 52, 419-434.

CLAUSEN, J. AND HANSEN, I. B. (1970) MYELIN CONSTITUENTS OF HUMAN CENTRAL NERVOUS SYSTEM. *ACTA NEUROL SCAND,* 46, 1-17.

COETZEE, T., FUJITA, N., DUPREE, J., SHI, R., BLIGHT, A., SUZUKI, K. AND POPKO, B. (1996) MYELINATION IN THE ABSENCE OF GALACTOCEREBROSIDE AND SULFATIDE: NORMAL STRUCTURE WITH ABNORMAL FUNCTION AND REGIONAL INSTABILITY. *CELL,* 86, 209-219.

COGAN, D. G., KUWABARA, T., KOLODNY, E. AND DRISCOLL, S. (1984) GANGLIOSIDOSES AND THE FETAL RETINA. *OPHTHALMOLOGY,* 91, 508-512.

CRAIG AND CLARKE (1959) METABOLIC NEUROVISCERAL DISORDER WITH ACCUMULATION OF AN UNIDENTIFIED SUBSTANCE: VARIANT OF HURLER'S SYNDROME. *AMERICAN JOURNAL OF DISEASES OF CHILDREN,* 98, 577.

CUZNER, M. L. AND DAVISON, A. N. (1968) THE LIPID COMPOSITION OF RAT BRAIN MYELIN AND SUBCELLULAR FRACTIONS DURING DEVELOPMENT. *BIOCHEM J,* 106, 29-34.

D'ANGELO, G., CAPASSO, S., STICCO, L. AND RUSSO, D. (2013) GLYCOSPHINGOLIPIDS: SYNTHESIS AND FUNCTIONS. *FEBS J,* 280, 6338-6353.

DAS, S. K., STEEN, M. E., MCCULLOUGH, M. S. AND BHATTACHARYYA, D. K. (1978) COMPOSITION OF LIPIDS OF BOVINE OPTIC NERVE. *LIPIDS,* 13, 679-684.

DAVIES, L. R., PEARCE, O. M., TESSIER, M. B. *ET AL.* (2012) METABOLISM OF VERTEBRATE AMINO SUGARS WITH N-GLYCOLYL GROUPS: RESISTANCE OF ALPHA2-8-LINKED N-GLYCOLYLNEURAMINIC ACID TO ENZYMATIC CLEAVAGE. *J BIOL CHEM,* 287, 28917-28931.

DENNY, C. A., ALROY, J., PAWLYK, B. S., SANDBERG, M. A., D'AZZO, A. AND SEYFRIED, T. N. (2007) NEUROCHEMICAL, MORPHOLOGICAL, AND NEUROPHYSIOLOGICAL ABNORMALITIES IN RETINAS OF SANDHOFF AND GM1 GANGLIOSIDOSIS MICE. *J NEUROCHEM,* 101, 1294-1302.

DI ROCCO, M., ROSSI, A., PARENTI, G., ALLEGRI, A. E., FILOCAMO, M., PESSAGNO, A., TORTORI-DONATI, P., MINETTI, C. AND BIANCHERI, R. (2005) DIFFERENT MOLECULAR MECHANISMS LEADING TO WHITE MATTER HYPOMYELINATION IN INFANTILE ONSET LYSOSOMAL DISORDERS. *NEUROPEDIATRICS,* 36, 265-269.

EMERY, J. M., GREEN, W. R., WYLLIE, R. G. AND HOWELL, R. R. (1971) GM1-GANGLIOSIDOSIS. OCULAR AND PATHOLOGICAL MANIFESTATIONS. *ARCH OPHTHALMOL,* 85, 177-187.

FAROOQUI, A. A. AND HORROCKS, L. A. (2001) PLASMALOGENS: WORKHORSE LIPIDS OF MEMBRANES IN NORMAL AND INJURED NEURONS AND GLIA. *NEUROSCIENTIST,* 7, 232-245.

FAROOQUI, A. A., ONG, W. Y. AND HORROCKS, L. A. (2006) INHIBITORS OF BRAIN PHOSPHOLIPASE A2 ACTIVITY: THEIR NEUROPHARMACOLOGICAL EFFECTS AND THERAPEUTIC IMPORTANCE FOR THE TREATMENT OF NEUROLOGIC DISORDERS. *PHARMACOL REV,* 58, 591-620.

FOLCH, J., LEES, M. AND SLOANE STANLEY, G. H. (1957) A SIMPLE METHOD FOR THE ISOLATION AND PURIFICATION OF TOTAL LIPIDES FROM ANIMAL TISSUES. *J BIOL CHEM,* 226, 497-509.

FOLKERTH, R. D., ALROY, J., BHAN, I. AND KAYE, E. M. (2000) INFANTILE G(M1) GANGLIOSIDOSIS: COMPLETE MORPHOLOGY AND HISTOCHEMISTRY OF TWO AUTOPSY CASES, WITH PARTICULAR REFERENCE TO DELAYED CENTRAL NERVOUS SYSTEM MYELINATION. *PEDIATR DEV PATHOL,* 3, 73-86.

FREEZE, H. H. AND NG, B. G. (2011) GOLGI GLYCOSYLATION AND HUMAN INHERITED DISEASES. *COLD SPRING HARB PERSPECT BIOL,* 3, A005371.

FURUYA, S., IRIE, F., HASHIKAWA, T., NAKAZAWA, K., KOZAKAI, A., HASEGAWA, A., SUDO, K. AND HIRABAYASHI, Y. (1994) GANGLIOSIDE GD1 ALPHA IN CEREBELLAR PURKINJE CELLS. ITS SPECIFIC ABSENCE IN MOUSE MUTANTS WITH PURKINJE CELL ABNORMALITY AND ALTERED IMMUNOREACTIVITY IN RESPONSE TO CONJUNCTIVE STIMULI CAUSING LONG-TERM DESENSITIZATION. *J BIOL CHEM,* 269, 32418-32425.

GANSER, A. L., KERNER, A. L., BROWN, B. J., DAVISSON, M. T. AND KIRSCHNER, D. A. (1988) A SURVEY OF NEUROLOGICAL MUTANT MICE. II. LIPID COMPOSITION OF MYELINATED TISSUE IN POSSIBLE MYELIN MUTANTS. *DEV NEUROSCI,* 10, 123-140.

GANSER, A. L. AND KIRSCHNER, D. A. (1984) DIFFERENTIAL EXPRESSION OF GANGLIOSIDES ON THE SURFACES OF MYELINATED NERVE FIBERS. *J NEUROSCI RES,* 12, 245-255.

GUMPEL, M., GOUT, O., LUBETZKI, C., GANSMULLER, A. AND BAUMANN, N. (1989) MYELINATION AND REMYELINATION IN THE CENTRAL NERVOUS SYSTEM BY TRANSPLANTED OLIGODENDROCYTES USING THE SHIVERER MODEL. DISCUSSION ON THE REMYELINATING CELL POPULATION IN ADULT MAMMALS. *DEV NEUROSCI,* 11, 132-139.

GURURAJ, A., SZTRIHA, L., HERTECANT, J., JOHANSEN, J. G., GEORGIOU, T., CAMPOS, Y., DROUSIOTOU, A. AND D'AZZO, A. (2005) MAGNETIC RESONANCE IMAGING FINDINGS AND NOVEL MUTATIONS IN GM1 GANGLIOSIDOSIS. *J CHILD NEUROL,* 20, 57-60.

HAHN, C. N., DEL PILAR MARTIN, M., SCHRODER, M., VANIER, M. T., HARA, Y., SUZUKI, K. AND D'AZZO, A. (1997) GENERALIZED CNS DISEASE AND MASSIVE GM1-GANGLIOSIDE ACCUMULATION IN MICE

DEFECTIVE IN LYSOSOMAL ACID BETA-GALACTOSIDASE. *HUM MOL GENET,* 6, 205-211.

HAKOMORI, S. (1990) BIFUNCTIONAL ROLE OF GLYCOSPHINGOLIPIDS. MODULATORS FOR TRANSMEMBRANE SIGNALING AND MEDIATORS FOR CELLULAR INTERACTIONS. *J BIOL CHEM,* 265, 18713-18716.

HAMA, H. (2010) FATTY ACID 2-HYDROXYLATION IN MAMMALIAN SPHINGOLIPID BIOLOGY. *BIOCHIM BIOPHYS ACTA,* 1801, 405-414.

HARLALKA, G. V., LEHMAN, A., CHIOZA, B. *ET AL.* (2013) MUTATIONS IN B4GALNT1 (GM2 SYNTHASE) UNDERLIE A NEW DISORDER OF GANGLIOSIDE BIOSYNTHESIS. *BRAIN,* 136, 3618-3624.

HAUSER, E. C., KASPERZYK, J. L., D'AZZO, A. AND SEYFRIED, T. N. (2004) INHERITANCE OF LYSOSOMAL ACID BETA-GALACTOSIDASE ACTIVITY AND GANGLIOSIDES IN CROSSES OF DBA/2J AND KNOCKOUT MICE. *BIOCHEM GENET,* 42, 241-257.

HAYASHI, A., KANEKO, N., TOMIHIRA, C. AND BABA, H. (2013) SULFATIDE DECREASE IN MYELIN INFLUENCES FORMATION OF THE PARANODAL AXO-GLIAL JUNCTION AND CONDUCTION VELOCITY IN THE SCIATIC NERVE. *GLIA,* 61, 466-474.

HEINECKE, K. A., PEACOCK, B. N., BLAZAR, B. R., TOLAR, J. AND SEYFRIED, T. N. (2011) LIPID COMPOSITION OF WHOLE BRAIN AND CEREBELLUM IN HURLER SYNDROME (MPS IH) MICE. *NEUROCHEM RES,* 36, 1669-1676.

HOLM, H. (1972) GANGLIOSIDES OF THE OPTIC PATHWAY: BIOSYNTHESIS AND BIODEGRADATION STUDIED IN VIVO. *J NEUROCHEM,* 19, 623-629.

HOLM, M. AND MANSSON, J. E. (1974) GANGLIOSIDES OF BOVINE OPTIC NERVE. *FEBS LETT,* 45, 159-161.

HORROCKS, L. A. (1973) COMPOSITION AND METABOLISM OF MYELIN PHOSPHOGLYCERIDES DURING MATURATION AND AGING. *PROG BRAIN RES,* 40, 383-395.

INOUYE, H., GANSER, A. L. AND KIRSCHNER, D. A. (1985) SHIVERER AND NORMAL PERIPHERAL MYELIN COMPARED: BASIC PROTEIN LOCALIZATION, MEMBRANE INTERACTIONS, AND LIPID COMPOSITION. *J NEUROCHEM,* 45, 1911-1922.

ISHIBASHI, T., DUPREE, J. L., IKENAKA, K. *ET AL.* (2002) A MYELIN GALACTOLIPID, SULFATIDE, IS ESSENTIAL FOR MAINTENANCE OF

ION CHANNELS ON MYELINATED AXON BUT NOT ESSENTIAL FOR INITIAL CLUSTER FORMATION. *J NEUROSCI,* 22, 6507-6514.

IWAMASA, T., OHSHITA, T., NASHIRO, K. AND IWANAGA, M. (1987) DEMONSTRATION OF GM1-GANGLIOSIDE IN NERVOUS SYSTEM IN GENERALIZED GM1-GANGLIOSIDOSIS USING CHOLERA TOXIN B SUBUNIT. *ACTA NEUROPATHOL,* 73, 357-360.

JACKMAN, N., ISHII, A. AND BANSAL, R. (2009) OLIGODENDROCYTE DEVELOPMENT AND MYELIN BIOGENESIS: PARSING OUT THE ROLES OF GLYCOSPHINGOLIPIDS. *PHYSIOLOGY (BETHESDA),* 24, 290-297.

JAIN, A., KOHLI, A. AND SACHAN, D. (2010) INFANTILE SANDHOFF'S DISEASE WITH PERIPHERAL NEUROPATHY. *PEDIATR NEUROL,* 42, 459-461.

JENNEMANN, R., SANDHOFF, R., WANG, S. *ET AL.* (2005) CELL-SPECIFIC DELETION OF GLUCOSYLCERAMIDE SYNTHASE IN BRAIN LEADS TO SEVERE NEURAL DEFECTS AFTER BIRTH. *PROC NATL ACAD SCI U S A,* 102, 12459-12464.

JEYAKUMAR, M., THOMAS, R., ELLIOT-SMITH, E. *ET AL.* (2003) CENTRAL NERVOUS SYSTEM INFLAMMATION IS A HALLMARK OF PATHOGENESIS IN MOUSE MODELS OF GM1 AND GM2 GANGLIOSIDOSIS. *BRAIN,* 126, 974-987.

KARBE, E. (1973) ANIMAL MODEL OF HUMAN DISEASE GM2-GANGLIOSIDOSES (AMAUROTIC IDIOCIES) TYPES I, II, AND 3. *AM J PATHOL,* 71, 151-154.

KARTHIGASAN, J., EVANS, E. L., VOUYIOUKLIS, D. A., INOUYE, H., BORENSHTEYN, N., RAMAMURTHY, G. V. AND KIRSCHNER, D. A. (1996) EFFECTS OF RUMPSHAKER MUTATION ON CNS MYELIN COMPOSITION AND STRUCTURE. *J NEUROCHEM,* 66, 338-345.

KASAMA, T. AND TAKETOMI, T. (1986) ABNORMALITIES OF CEREBRAL LIPIDS IN GM1-GANGLIOSIDOSES, INFANTILE, JUVENILE, AND CHRONIC TYPE. *JPN J EXP MED,* 56, 1-11.

KASPERZYK, J. L., D'AZZO, A., PLATT, F. M., ALROY, J. AND SEYFRIED, T. N. (2005) SUBSTRATE REDUCTION REDUCES GANGLIOSIDES IN POSTNATAL CEREBRUM-BRAINSTEM AND CEREBELLUM IN GM1 GANGLIOSIDOSIS MICE. *J LIPID RES,* 46, 744-751.

KASPERZYK, J. L., EL-ABBADI, M. M., HAUSER, E. C., D'AZZO, A., PLATT, F. M. AND SEYFRIED, T. N. (2004) N-BUTYLDEOXYGALACTONOJIRIMYCIN

REDUCES NEONATAL BRAIN GANGLIOSIDE CONTENT IN A MOUSE MODEL OF GM1 GANGLIOSIDOSIS. *J NEUROCHEM,* 89, 645-653.

KAWANO, T., KOYAMA, S., TAKEMATSU, H., KOZUTSUMI, Y., KAWASAKI, H., KAWASHIMA, S., KAWASAKI, T. AND SUZUKI, A. (1995) MOLECULAR CLONING OF CYTIDINE MONOPHOSPHO-N-ACETYLNEURAMINIC ACID HYDROXYLASE. REGULATION OF SPECIES- AND TISSUE-SPECIFIC EXPRESSION OF N-GLYCOLYLNEURAMINIC ACID. *J BIOL CHEM,* 270, 16458-16463.

KAYE, E. M., ALROY, J., RAGHAVAN, S. S., SCHWARTING, G. A., ADELMAN, L. S., RUNGE, V., GELBLUM, D., THALHAMMER, J. G. AND ZUNIGA, G. (1992) DYSMYELINOGENESIS IN ANIMAL MODEL OF GM1 GANGLIOSIDOSIS. *PEDIATR NEUROL,* 8, 255-261.

KETTENMANN, H. AND VERKHRATSKY, A. (2011) ADAPTED FROM: NEUROGLIA - LIVING NERVE GLUE HTTP://WWW.NETWORKGLIA.EU/EN/OLIGODENDROCYTES.

KIRSCHNER, D. A., AVILA, R. L., GAMEZ SAZO, R. E. *ET AL.* (2010) RAPID ASSESSMENT OF INTERNODAL MYELIN INTEGRITY IN CENTRAL NERVOUS SYSTEM TISSUE. *J NEUROSCI RES,* 88, 712-721.

KIRSCHNER, D. A. AND SIDMAN, R. L. (1976) X-RAY DIFFRACTION STUDY OF MYELIN STRUCTURE IN IMMATURE AND MUTANT MICE. *BIOCHIM BIOPHYS ACTA,* 448, 73-87.

KIRSCHNER, D. A., SZUMOWSKI, K., GABREELS-FESTEN, A. A., HOOGENDIJK, J. E. AND BOLHUIS, P. A. (1996) INHERITED DEMYELINATING PERIPHERAL NEUROPATHIES: RELATING MYELIN PACKING ABNORMALITIES TO P0 MOLECULAR DEFECTS. *J NEUROSCI RES,* 46, 502-508.

KOLESNICK, R. AND HANNUN, Y. A. (1999) CERAMIDE AND APOPTOSIS. *TRENDS BIOCHEM SCI,* 24, 224-225; AUTHOR REPLY 227.

KOLTER, T. (2012) GANGLIOSIDE BIOCHEMISTRY. *ISRN BIOCHEMISTRY,* 2012, 36.

KOLTER, T., PROIA, R. L. AND SANDHOFF, K. (2002) COMBINATORIAL GANGLIOSIDE BIOSYNTHESIS. *J BIOL CHEM,* 277, 25859-25862.

KOLTER, T. AND SANDHOFF, K. (1998) GLYCOSPHINGOLIPID DEGRADATION AND ANIMAL MODELS OF GM2-GANGLIOSIDOSES. *J INHERIT METAB DIS,* 21, 548-563.

KOLTER, T. AND SANDHOFF, K. (2006) SPHINGOLIPID METABOLISM DISEASES. *BIOCHIM BIOPHYS ACTA,* 1758, 2057-2079.

KROLL, R. A., PAGEL, M. A., ROMAN-GOLDSTEIN, S., BARKOVICH, A. J., D'AGOSTINO, A. N. AND NEUWELT, E. A. (1995) WHITE MATTER CHANGES ASSOCIATED WITH FELINE GM2 GANGLIOSIDOSIS (SANDHOFF DISEASE): CORRELATION OF MR FINDINGS WITH PATHOLOGIC AND ULTRASTRUCTURAL ABNORMALITIES. *AJNR AM J NEURORADIOL,* 16, 1219-1226.

LANDING, B. H., SILVERMAN, F. N., CRAIG, J. M., JACOBY, M. D., LAHEY, M. E. AND CHADWICK, D. L. (1964) FAMILIAL NEUROVISCERAL LIPIDOSIS. AN ANALYSIS OF EIGHT CASES OF A SYDROME PREVIOUSLY REPORTED AS "HURLER-VARIENT," "PSEUDO-HURLER," AND "TAY-SACHS DISEASE WITH VISCERAL INVOLVEMENT" *AM J DIS CHILD,* 108, 503-522.

LEDEEN, R. (1983) GANGLIOSIDES. IN: *HANDBOOK OF NEUROCHEMISTRY*, (L. A ED.), VOL. 3. PLENUM PRESS, NEW YORK.

LEDEEN, R. W. AND YU, R. K. (1982) GANGLIOSIDES: STRUCTURE, ISOLATION, AND ANALYSIS. *METHODS ENZYMOL,* 83, 139-191.

LINGWOOD, C. A. (2011) GLYCOSPHINGOLIPID FUNCTIONS. *COLD SPRING HARB PERSPECT BIOL,* 3.

LUPACHYK, S., WATCHO, P., OBROSOV, A. A., STAVNIICHUK, R. AND OBROSOVA, I. G. (2013) ENDOPLASMIC RETICULUM STRESS CONTRIBUTES TO PREDIABETIC PERIPHERAL NEUROPATHY. *EXP NEUROL,* 247, 342-348.

LYON GL, ADAM RD AND EH, K. (1996) NEUROLOGY OF HEREDITARY METABOLIC DISEASES OF CHILDREN IN: *NEUROLOGY OF HEREDITARY METABOLIC DISEASES OF CHILDREN* PP. 53-55. MCGRAW-HILL PROFESSIONAL PUBLISHING.

MACALA, L. J., YU, R. K. AND ANDO, S. (1983) ANALYSIS OF BRAIN LIPIDS BY HIGH PERFORMANCE THIN-LAYER CHROMATOGRAPHY AND DENSITOMETRY. *J LIPID RES,* 24, 1243-1250.

MACBRINN, M. C. AND O'BRIEN, J. S. (1969) LIPID COMPOSITION OF OPTIC NERVE MYELIN. *J NEUROCHEM,* 16, 7-12.

MARCUS, J., HONIGBAUM, S., SHROFF, S., HONKE, K., ROSENBLUTH, J. AND DUPREE, J. L. (2006) SULFATIDE IS ESSENTIAL FOR THE

MAINTENANCE OF CNS MYELIN AND AXON STRUCTURE. *GLIA,* 53, 372-381.

MATEU, L., LUZZATI, V., BORGO, M., VONASEK, E. AND VARGAS, R. (1991) ORDER-DISORDER PHENOMENA IN MYELINATED NERVE SHEATHS. III. THE STRUCTURE OF MYELIN IN RAT OPTIC NERVES OVER THE COURSE OF MYELINOGENESIS. *J MOL BIOL,* 220, 351-357.

MATSUDA, J., SUZUKI, O., OSHIMA, A., OGURA, A., NAIKI, M. AND SUZUKI, Y. (1997A) NEUROLOGICAL MANIFESTATIONS OF KNOCKOUT MICE WITH BETA-GALACTOSIDASE DEFICIENCY. *BRAIN DEV,* 19, 19-20.

MATSUDA, J., SUZUKI, O., OSHIMA, A. *ET AL.* (1997B) BETA-GALACTOSIDASE-DEFICIENT MOUSE AS AN ANIMAL MODEL FOR GM1-GANGLIOSIDOSIS. *GLYCOCONJ J,* 14, 729-736.

MCNALLY, M. A., BAEK, R. C., AVILA, R. L., SEYFRIED, T. N., STRICHARTZ, G. R. AND KIRSCHNER, D. A. (2007) PERIPHERAL NERVOUS SYSTEM MANIFESTATIONS IN A SANDHOFF DISEASE MOUSE MODEL: NERVE CONDUCTION, MYELIN STRUCTURE, LIPID ANALYSIS. *J NEGAT RESULTS BIOMED,* 6, 8.

MEIKLE, P. J., HOPWOOD, J. J., CLAGUE, A. E. AND CAREY, W. F. (1999) PREVALENCE OF LYSOSOMAL STORAGE DISORDERS. *JAMA,* 281, 249-254.

MENKES, J. H., PHILIPPART, M. AND CONCONE, M. C. (1966) CONCENTRATION AND FATTY ACID COMPOSITION OF CEREBROSIDES AND SULFATIDES IN MATURE AND IMMATURE HUMAN BRAIN. *J LIPID RES,* 7, 479-486.

MICU, I., JIANG, Q., CODERRE, E. *ET AL.* (2006) NMDA RECEPTORS MEDIATE CALCIUM ACCUMULATION IN MYELIN DURING CHEMICAL ISCHAEMIA. *NATURE,* 439, 988-992.

MIN, Y., KRISTIANSEN, K., BOGGS, J. M., HUSTED, C., ZASADZINSKI, J. A. AND ISRAELACHVILI, J. (2009) INTERACTION FORCES AND ADHESION OF SUPPORTED MYELIN LIPID BILAYERS MODULATED BY MYELIN BASIC PROTEIN. *PROC NATL ACAD SCI U S A,* 106, 3154-3159.

MONDELLI, M., ROSSI, A., PALMERI, S., RIZZUTO, N. AND FEDERICO, A. (1989) NEUROPHYSIOLOGICAL STUDY IN CHRONIC GM2 GANGLIOSIDOSIS (HEXOSAMINIDASE A AND B DEFICIENCY), WITH MOTOR NEURON DISEASE PHENOTYPE. *ITAL J NEUROL SCI,* 10, 433-439.

MULLER, G., ALLDINGER, S., MORITZ, A., ZURBRIGGEN, A., KIRCHHOF, N., SEWELL, A. AND BAUMGARTNER, W. (2001) GM1-GANGLIOSIDOSIS IN ALASKAN HUSKIES: CLINICAL AND PATHOLOGIC FINDINGS. *VET PATHOL,* 38, 281-290.

MURRAY, J. A., BLAKEMORE, W. F. AND BARNETT, K. C. (1977) OCULAR LESIONS IN CATS WITH GM1-GANGLIOSIDOSIS WITH VISCERAL INVOLVEMENT. *J SMALL ANIM PRACT,* 18, 1-10.

MUSE, E. D., JUREVICS, H., TOEWS, A. D., MATSUSHIMA, G. K. AND MORELL, P. (2001) PARAMETERS RELATED TO LIPID METABOLISM AS MARKERS OF MYELINATION IN MOUSE BRAIN. *J NEUROCHEM,* 76, 77-86.

MUTHUPALANI, S., TORRES, P.A., WANG, B.C., ZENG, B.J., EATON,, S., E., I., DUCORE, R., MAGANTI, R., KEATING, J., PERRY, B.J., TSENG, F.S.,WALISZEWSKI,, N., P., M., CAUSEY, R., SEGER, R., MARCH, P., TIDWELL, A., PFANNL, R., SEYFRIED, AND T., K., E.H. & ALROY, J. (2014) GM1-GANGLIOSIDOSIS IN AMERICAN BLACK BEARS: CLINICAL, PATHOLOGICAL, BIOCHEMICAL AND MOLECULAR GENETIC CHARACTERIZATION. *MOLECULAR GENETICS AND METABOLISM*.

MUTKA, A. L., HAAPANEN, A., KAKELA, R. *ET AL.* (2010) MURINE CATHEPSIN D DEFICIENCY IS ASSOCIATED WITH DYSMYELINATION/MYELIN DISRUPTION AND ACCUMULATION OF CHOLESTERYL ESTERS IN THE BRAIN. *J NEUROCHEM,* 112, 193-203.

NADA, R., GUPTA, K., LAL, S. B. AND VASISHTA, R. K. (2011) AN AUTOPSY CASE OF INFANTILE GM1 GANGLIOSIDOSIS WITH ADRENAL CALCIFICATION. *METAB BRAIN DIS,* 26, 307-310.

NATURE (2013) SPECIALIZED MEMBRANES ORGANIZE THE EUKARYOTIC CELL CYTOPLASM INTO COMPARTMENTS HTTP://WWW.NATURE.COM/SCITABLE/EBOOKS/ESSENTIALS-OF-CELL-BIOLOGY-14749010/112300712. IN: *CONTENTS OF ESSENTIALS OF CELL BIOLOGY*.

NINDS (2011) GENERALIZED GANGLIOSIDOSES HTTP://WWW.NINDS.NIH.GOV/DISORDERS/GANGLIOSIDOSES/GANGLIOSIDOSES.HTM.

NORMAN, R. M., URICH, H., TINGEY, A. H. AND GOODBODY, R. A. (1959) TAY-SACHS' DISEASE WITH VISCERAL INVOLVEMENT AND ITS RELATIONSHIP TO NIEMANN-PICK'S DISEASE. *J PATHOL BACTERIOL,* 78, 409-421.

NUSSBAUM, J. L., NESKOVIC, N. AND MANDEL, P. (1971) THE FATTY ACID COMPOSITION OF PHOSPHOLIPIDS AND GLYCOLIPIDS IN JIMPY MOUSE BRAIN. *J NEUROCHEM,* 18, 1529-1543.

O'BRIEN, J. S. AND SAMPSON, E. L. (1965A) FATTY ACID AND FATTY ALDEHYDE COMPOSITION OF THE MAJOR BRAIN LIPIDS IN NORMAL HUMAN GRAY MATTER, WHITE MATTER, AND MYELIN. *J LIPID RES,* 6, 545-551.

O'BRIEN, J. S. AND SAMPSON, E. L. (1965B) LIPID COMPOSITION OF THE NORMAL HUMAN BRAIN: GRAY MATTER, WHITE MATTER, AND MYELIN. *J LIPID RES,* 6, 537-544.

O'BRIEN, J. S., SAMPSON, E. L. AND STERN, M. B. (1967) LIPID COMPOSITION OF MYELIN FROM THE PERIPHERAL NERVOUS SYSTEM. INTRADURAL SPINAL ROOTS. *J NEUROCHEM,* 14, 357-365.

O'BRIEN, J. S., STERN, M. B., LANDING, B. H., O'BRIEN, J. K. AND DONNELL, G. N. (1965C) GENERALIZED GANGLIOSIDOSIS: ANOTHER INBORN ERROR OF GANGLIOSIDE METABOLISM? *AM J DIS CHILD,* 109, 338-346.

OKADA, S. AND O'BRIEN, J. S. (1968) GENERALIZED GANGLIOSIDOSIS: BETA-GALACTOSIDASE DEFICIENCY. *SCIENCE,* 160, 1002-1004.

PAINTLIA, A. S., GILG, A. G., KHAN, M., SINGH, A. K., BARBOSA, E. AND SINGH, I. (2003) CORRELATION OF VERY LONG CHAIN FATTY ACID ACCUMULATION AND INFLAMMATORY DISEASE PROGRESSION IN CHILDHOOD X-ALD: IMPLICATIONS FOR POTENTIAL THERAPIES. *NEUROBIOL DIS,* 14, 425-439.

PLATT, F. M., BOLAND, B. AND VAN DER SPOEL, A. C. (2012) THE CELL BIOLOGY OF DISEASE: LYSOSOMAL STORAGE DISORDERS: THE CELLULAR IMPACT OF LYSOSOMAL DYSFUNCTION. *J CELL BIOL,* 199, 723-734.

POLIAK, S. AND PELES, E. (2003) THE LOCAL DIFFERENTIATION OF MYELINATED AXONS AT NODES OF RANVIER. *NAT REV NEUROSCI,* 4, 968-980.

READ, D. H., HARRINGTON, D. D., KEENANA, T. W. AND HINSMAN, E. J. (1976) NEURONAL-VISCERAL GM1 GANGLIOSIDOSIS IN A DOG WITH BETA-GALACTOSIDASE DEFICIENCY. *SCIENCE,* 194, 442-445.

RUOCCO, M. J. AND SHIPLEY, G. G. (1984) INTERACTION OF CHOLESTEROL WITH GALACTOCEREBROSIDE AND GALACTOCEREBROSIDE-

PHOSPHATIDYLCHOLINE BILAYER MEMBRANES. *BIOPHYS J,* 46, 695-707.

SALMOND, R. J., LUROSS, J. A. AND WILLIAMS, N. A. (2002) IMMUNE MODULATION BY THE CHOLERA-LIKE ENTEROTOXINS. *EXPERT REV MOL MED,* 4, 1-16.

SANDHOFF, K. AND HARZER, K. (2013) GANGLIOSIDES AND GANGLIOSIDOSES: PRINCIPLES OF MOLECULAR AND METABOLIC PATHOGENESIS. *J NEUROSCI,* 33, 10195-10208.

SANDHOFF, K. AND VAN ECHTEN, G. (1994) GANGLIOSIDE METABOLISM: ENZYMOLOGY, TOPOLOGY AND REGULATION. *PROG BRAIN RES,* 101, 17-29.

SAUNDERS, G. K., WOOD, P. A., MYERS, R. K., SHELL, L. G. AND CARITHERS, R. (1988) GM1 GANGLIOSIDOSIS IN PORTUGUESE WATER DOGS: PATHOLOGIC AND BIOCHEMICAL FINDINGS. *VET PATHOL,* 25, 265-269.

SCHMITT, F. O., BEAR, R. S. AND CLARK, G. L. (1935) THE ROLE OF LIPOIDS IN THE X-RAY DIFFRACTION PATTERNS OF NERVE *SCIENCE,* 82, 44-45.

SCHNAAR, R. L. (2010) BRAIN GANGLIOSIDES IN AXON-MYELIN STABILITY AND AXON REGENERATION. *FEBS LETT,* 584, 1741-1747.

SCHNAAR RL, SUZUKI A AND P., S. (2009) CHAPTER 10. GLYCOSPHINGOLIPIDS HTTP://WWW.NCBI.NLM.NIH.GOV/BOOKS/NBK1909/. IN: *ESSENTIALS OF GLYCOBIOLOGY*, (C. R. VARKI A, ESKO JD, ET AL., EDITORS ED.). COLD SPRING HARBOR LABORATORY PRESS, COLD SPRING HARBOR.

SEYFRIED, T. N., BERNARD, D. J. AND YU, R. K. (1984A) CELLULAR DISTRIBUTION OF GANGLIOSIDES IN THE DEVELOPING MOUSE CEREBELLUM: ANALYSIS USING THE STAGGERER MUTANT. *J NEUROCHEM,* 43, 1152-1162.

SEYFRIED, T. N., GLASER, G. H. AND YU, R. K. (1978) CEREBRAL, CEREBELLAR, AND BRAIN STEM GANGLIOSIDES IN MICE SUSCEPTIBLE TO AUDIOGENIC SEIZURES. *J NEUROCHEM,* 31, 21-27.

SEYFRIED, T. N., HEINECKE, K. A., MANTIS, J. G. AND DENNY, C. A. (2009) BRAIN LIPID ANALYSIS IN MICE WITH RETT SYNDROME. *NEUROCHEM RES,* 34, 1057-1065.

SEYFRIED, T. N., MIYAZAWA, N. AND YU, R. K. (1983) CELLULAR LOCALIZATION OF GANGLIOSIDES IN THE DEVELOPING MOUSE

CEREBELLUM: ANALYSIS USING THE WEAVER MUTANT. *J NEUROCHEM,* 41, 491-505.

SEYFRIED, T. N. AND YU, R. K. (1980) HETEROSIS FOR BRAIN MYELIN CONTENT IN MICE. *BIOCHEM GENET,* 18, 1229-1237.

SEYFRIED, T. N. AND YU, R. K. (1984B) CELLULAR LOCALIZATION OF GANGLIOSIDES IN THE MOUSE CEREBELLUM: ANALYSIS USING NEUROLOGICAL MUTANTS. *ADV EXP MED BIOL,* 174, 169-181.

SEYFRIED, T. N. AND YU, R. K. (1990) CEREBELLAR GANGLIOSIDE ABNORMALITIES IN PCD MUTANT MICE. *J NEUROSCI RES,* 26, 105-111.

SEYFRIED, T. N., YU, R. K. AND MIYAZAWA, N. (1982) DIFFERENTIAL CELLULAR ENRICHMENT OF GANGLIOSIDES IN THE MOUSE CEREBELLUM: ANALYSIS USING NEUROLOGICAL MUTANTS. *J NEUROCHEM,* 38, 551-559.

SHAPIRO, B. E., LOGIGIAN, E. L., KOLODNY, E. H. AND PASTORES, G. M. (2008) LATE-ONSET TAY-SACHS DISEASE: THE SPECTRUM OF PERIPHERAL NEUROPATHY IN 30 AFFECTED PATIENTS. *MUSCLE NERVE,* 38, 1012-1015.

SHEAHAN, B. J., DONNELLY, W. J. AND GRIMES, T. D. (1978) OCULAR PATHOLOGY OF BOVINE GM1 GANGLIOSIDOSIS. *ACTA NEUROPATHOL,* 41, 91-95.

SHEIKH, K. A., SUN, J., LIU, Y., KAWAI, H., CRAWFORD, T. O., PROIA, R. L., GRIFFIN, J. W. AND SCHNAAR, R. L. (1999) MICE LACKING COMPLEX GANGLIOSIDES DEVELOP WALLERIAN DEGENERATION AND MYELINATION DEFECTS. *PROC NATL ACAD SCI U S A,* 96, 7532-7537.

SHEN, W. C., TSAI, F. J. AND TSAI, C. H. (1998) MYELINATION ARREST DEMONSTRATED USING MAGNETIC RESONANCE IMAGING IN A CHILD WITH TYPE I GM1 GANGLIOSIDOSIS. *J FORMOS MED ASSOC,* 97, 296-299.

SHIN, M. K., JUNG, W. R., KIM, H. G., ROH, S. E., KWAK, C. H., KIM, C. H., KIM, S. J. AND KIM, K. L. (2014) THE GANGLIOSIDE GQ1B REGULATES BDNF EXPRESSION VIA THE NMDA RECEPTOR SIGNALING PATHWAY. *NEUROPHARMACOLOGY,* 77, 414-421.

SINGH, A. K., HARRISON, S. H. AND SCHOENIGER, J. S. (2000) GANGLIOSIDES AS RECEPTORS FOR BIOLOGICAL TOXINS: DEVELOPMENT OF SENSITIVE FLUOROIMMUNOASSAYS USING GANGLIOSIDE-BEARING LIPOSOMES. *ANAL CHEM,* 72, 6019-6024.

SINIGERSKA, I., CHANDLER, D., VAGHJIANI, V., HASSANOVA, I., GOODING, R., MORRONE, A., KREMENSKY, I. AND KALAYDJIEVA, L. (2006) FOUNDER MUTATION CAUSING INFANTILE GM1-GANGLIOSIDOSIS IN THE GYPSY POPULATION. *MOL GENET METAB,* 88, 93-95.

SONNINO, S., MAURI, L., CHIGORNO, V. AND PRINETTI, A. (2006) GANGLIOSIDES AS COMPONENTS OF LIPID MEMBRANE DOMAINS. *GLYCOBIOLOGY,* 17, 1R-13R.

SPRITZ, N., SINGH, H. AND GEYER, B. (1973) MYELIN FROM HUMAN PERIPHERAL NERVES. QUANTITATIVE AND QUALITATIVE STUDIES IN TWO AGE GROUPS. *J CLIN INVEST,* 52, 520-523.

STARETZ-CHACHAM, O., LANG, T. C., LAMARCA, M. E., KRASNEWICH, D. AND SIDRANSKY, E. (2009) LYSOSOMAL STORAGE DISORDERS IN THE NEWBORN. *PEDIATRICS,* 123, 1191-1207.

STURGILL, E. R., AOKI, K., LOPEZ, P. H. *ET AL.* (2012) BIOSYNTHESIS OF THE MAJOR BRAIN GANGLIOSIDES GD1A AND GT1B. *GLYCOBIOLOGY,* 22, 1289-1301.

SUCHER, N. J., LEI, S. Z. AND LIPTON, S. A. (1991) CALCIUM CHANNEL ANTAGONISTS ATTENUATE NMDA RECEPTOR-MEDIATED NEUROTOXICITY OF RETINAL GANGLION CELLS IN CULTURE. *BRAIN RES,* 551, 297-302.

SUSUKI, K., BABA, H., TOHYAMA, K., KANAI, K., KUWABARA, S., HIRATA, K., FURUKAWA, K., RASBAND, M. N. AND YUKI, N. (2007) GANGLIOSIDES CONTRIBUTE TO STABILITY OF PARANODAL JUNCTIONS AND ION CHANNEL CLUSTERS IN MYELINATED NERVE FIBERS. *GLIA,* 55, 746-757.

SUZUKI, K., PODUSLO, J. F. AND PODUSLO, S. E. (1968A) FURTHER EVIDENCE FOR A SPECIFIC GANGLIOSIDE FRACTION CLOSELY ASSOCIATED WITH MYELIN. *BIOCHIM BIOPHYS ACTA,* 152, 576-586.

SUZUKI, K., PODUSLO, S. E. AND NORTON, W. T. (1967) GANGLIOSIDES IN THE MYELIN FRACTION OF DEVELOPING RATS. *BIOCHIM BIOPHYS ACTA,* 144, 375-381.

SUZUKI, K., SUZUKI, K. AND CHEN, G. C. (1968B) GM1-GANGLIOSIDOSIS (GNERALIZED GANGLIOSIDOSIS). MORPHOLOGY AND CHEMICAL PATHOLOGY. *PATHOL EUR,* 3, 389-408.

SUZUKI, Y., NANBA, E., MATSUDA, J., OSHIMA;, A. AND HIGAKI, K. (2001) B-GALACTOSIDASE DEFICIENCY (B-GALACTOSIDOSIS): GM1 GANGLIOSIDOSIS AND MORQUIO B DISEASE. IN: *THE METABOIC & MOLECULAR BASES OF INHERITED DISEASE*, (S. C. S. WS, B. B, B. AL, V. D, K. KW AND V. B EDS.), PP. 3775-3809. MCGRAW-HILL, NEW YORK.

SVENNERHOLM, L. (1957) QUANTITATIVE ESTIMATION OF SIALIC ACIDS. II. A COLORIMETRIC RESORCINOL-HYDROCHLORIC ACID METHOD. *BIOCHIM BIOPHYS ACTA,* 24, 604-611.

SVENNERHOLM, L. AND STALLBERG-STENHAGEN, S. (1968) CHANGES IN THE FATTY ACID COMPOSITION OF CEREBROSIDES AND SULFATIDES OF HUMAN NERVOUS TISSUE WITH AGE. *J LIPID RES,* 9, 215-225.

TATEMATSU, M., IMAIDA, K., ITO, N., TOGARI, H., SUZUKI, Y. AND OGIU, T. (1981) SANDHOFF DISEASE. *ACTA PATHOL JPN,* 31, 503-512.

TESSITORE, A., DEL, P. M. M., SANO, R. *ET AL.* (2004) GM1-GANGLIOSIDE-MEDIATED ACTIVATION OF THE UNFOLDED PROTEIN RESPONSE CAUSES NEURONAL DEATH IN A NEURODEGENERATIVE GANGLIOSIDOSIS. *MOL CELL,* 15, 753-766.

VAJN, K., VILJETIC, B., DEGMECIC, I. V., SCHNAAR, R. L. AND HEFFER, M. (2013) DIFFERENTIAL DISTRIBUTION OF MAJOR BRAIN GANGLIOSIDES IN THE ADULT MOUSE CENTRAL NERVOUS SYSTEM. *PLOS ONE,* 8, E75720.

VAN DER VOORN, J. P., KAMPHORST, W., VAN DER KNAAP, M. S. AND POWERS, J. M. (2004) THE LEUKOENCEPHALOPATHY OF INFANTILE GM1 GANGLIOSIDOSIS: OLIGODENDROCYTIC LOSS AND AXONAL DYSFUNCTION. *ACTA NEUROPATHOL,* 107, 539-545.

VAN DER VOORN, J. P., POUWELS, P. J., KAMPHORST, W., POWERS, J. M., LAMMENS, M., BARKHOF, F. AND VAN DER KNAAP, M. S. (2005) HISTOPATHOLOGIC CORRELATES OF RADIAL STRIPES ON MR IMAGES IN LYSOSOMAL STORAGE DISORDERS. *AJNR AM J NEURORADIOL,* 26, 442-446.

VAN MEER, G., VOELKER, D. R. AND FEIGENSON, G. W. (2008) MEMBRANE LIPIDS: WHERE THEY ARE AND HOW THEY BEHAVE. *NAT REV MOL CELL BIOL,* 9, 112-124.

VARGAS, V., VARGAS, R., MATEU, L. AND LUZZATI, V. (1997) THE EFFECTS OF UNDERNUTRITION ON THE PHYSICAL ORGANIZATION OF RAT

SCIATIC MYELIN SHEATHS: AN X-RAY SCATTERING STUDY. *ANN N Y ACAD SCI,* 817, 368-371.

VIADER, A., SASAKI, Y., KIM, S., STRICKLAND, A., WORKMAN, C. S., YANG, K., GROSS, R. W. AND MILBRANDT, J. (2013) ABERRANT SCHWANN CELL LIPID METABOLISM LINKED TO MITOCHONDRIAL DEFICITS LEADS TO AXON DEGENERATION AND NEUROPATHY. *NEURON,* 77, 886-898.

VONASEK, E., MATEU, L., LUZZATI, V., MARQUEZ, G., VARGAS, R., CESPEDES, G., COTUA, M. AND BORGES, J. (2001) A REVERSIBLE ABNORMAL FORM OF MYELIN: AN X-RAY SCATTERING STUDY OF HUMAN SURAL AND RAT SCIATIC NERVES. *EUR BIOPHYS J,* 30, 11-16.

VYAS, A. A., PATEL, H. V., FROMHOLT, S. E., HEFFER-LAUC, M., VYAS, K. A., DANG, J., SCHACHNER, M. AND SCHNAAR, R. L. (2002) GANGLIOSIDES ARE FUNCTIONAL NERVE CELL LIGANDS FOR MYELIN-ASSOCIATED GLYCOPROTEIN (MAG), AN INHIBITOR OF NERVE REGENERATION. *PROC NATL ACAD SCI U S A,* 99, 8412-8417.

VYAS, A. A. AND SCHNAAR, R. L. (2001) BRAIN GANGLIOSIDES: FUNCTIONAL LIGANDS FOR MYELIN STABILITY AND THE CONTROL OF NERVE REGENERATION. *BIOCHIMIE,* 83, 677-682.

WATZLAWIK, J., WARRINGTON, A. E. AND RODRIGUEZ, M. (2010) IMPORTANCE OF OLIGODENDROCYTE PROTECTION, BBB BREAKDOWN AND INFLAMMATION FOR REMYELINATION. *EXPERT REV NEUROTHER,* 10, 441-457.

WEISS, M. J., KRILL, A. E., DAWSON, G., HINDMAN, J. AND COTLIER, E. (1973) GM1 GANGLIOSIDOSIS TYPE I. *AM J OPHTHALMOL,* 76, 999-1004.

WIEGANDT, H. (1995) THE CHEMICAL CONSTITUTION OF GANGLIOSIDES OF THE VERTEBRATE NERVOUS SYSTEM. *BEHAV BRAIN RES,* 66, 85-97.

WILKENING, G., LINKE, T., UHLHORN-DIERKS, G. AND SANDHOFF, K. (2000) DEGRADATION OF MEMBRANE-BOUND GANGLIOSIDE GM1. STIMULATION BY BIS(MONOACYLGLYCERO)PHOSPHATE AND THE ACTIVATOR PROTEINS SAP-B AND GM2-AP. *J BIOL CHEM,* 275, 35814-35819.

XU, Y. H., BARNES, S., SUN, Y. AND GRABOWSKI, G. A. (2010) MULTI-SYSTEM DISORDERS OF GLYCOSPHINGOLIPID AND GANGLIOSIDE METABOLISM. *J LIPID RES,* 51, 1643-1675.

YAMANO, T., SHIMADA, M., OKADA, S., YUTAKA, T., KATO, T., INUI, K., YABUUCHI, H., KANZAKI, S. AND KANDA, S. (1983) ULTRASTRUCTURAL STUDY ON NERVOUS SYSTEM OF FETUS WITH GM1-GANGLIOSIDOSIS TYPE 1. *ACTA NEUROPATHOL,* 61, 15-20.

YAMASHITA, T., WU, Y. P., SANDHOFF, R. *ET AL.* (2005) INTERRUPTION OF GANGLIOSIDE SYNTHESIS PRODUCES CENTRAL NERVOUS SYSTEM DEGENERATION AND ALTERED AXON-GLIAL INTERACTIONS. *PROC NATL ACAD SCI U S A,* 102, 2725-2730.

YAO, D., MCGONIGAL, R., BARRIE, J. A. *ET AL.* (2014) NEURONAL EXPRESSION OF GALNAC TRANSFERASE IS SUFFICIENT TO PREVENT THE AGE-RELATED NEURODEGENERATIVE PHENOTYPE OF COMPLEX GANGLIOSIDE-DEFICIENT MICE. *J NEUROSCI,* 34, 880-891.

YIN, X., BAEK, R. C., KIRSCHNER, D. A., PETERSON, A., FUJII, Y., NAVE, K. A., MACKLIN, W. B. AND TRAPP, B. D. (2006) EVOLUTION OF A NEUROPROTECTIVE FUNCTION OF CENTRAL NERVOUS SYSTEM MYELIN. *J CELL BIOL,* 172, 469-478.

YU, R. K., TSAI, Y. T. AND ARIGA, T. (2012) FUNCTIONAL ROLES OF GANGLIOSIDES IN NEURODEVELOPMENT: AN OVERVIEW OF RECENT ADVANCES. *NEUROCHEM RES,* 37, 1230-1244.

YU, R. K., UENO, K., GLASER, G. H. AND TOURTELLOTTE, W. W. (1982) LIPID AND PROTEIN ALTERATIONS OF SPINAL CORD AND CORD MYELIN OF MULTIPLE SCLEROSIS. *J NEUROCHEM,* 39, 464-477.

YU, R. K. AND YEN, S. I. (1975) GANGLIOSIDES IN DEVELOPING MOUSE BRAIN MYELIN. *J NEUROCHEM,* 25, 229-232.

ZALC, B., MONGE, M., DUPOUEY, P., HAUW, J. J. AND BAUMANN, N. A. (1981) IMMUNOHISTOCHEMICAL LOCALIZATION OF GALACTOSYL AND SULFOGALACTOSYL CERAMIDE IN THE BRAIN OF THE 30-DAY-OLD MOUSE. *BRAIN RES,* 211, 341-354.